

Louisiana Transportation Research



PB99-107898

Construction and Comparison of Louisiana's Conventional and Alternative Base Courses Under Accelerated Loading (Interim Report 1, Phase 1)

by

**J. M. Metcalf
S. Romanoschi
Li Yongqi**

LOUISIANA STATE UNIVERSITY

and


M. Rasoulia

LOUISIANA TRANSPORTATION RESEARCH CENTER

LTRC

Louisiana Transportation Research Center

Sponsored Jointly by Louisiana State University and the Louisiana Department of Transportation and Development

1. Report No. FHWA/LA.88/312		 PB99-107898		3. Recipient's Catalog No.
4. Title and Subtitle Construction and Comparison of Louisiana's Conventional and Alternative Base Courses Under Accelerated Loading Interim Report 1, Phase 1		5. Report Date August 1998		
		6. Performing Organization Code		
7. Author(s) J.B. Metcalf, M. Rasoulia, S. Romanochi and Li Yongqi		8. Performing Organization Report No. 312		
9. Performing Organization Name and Address Institute of Recyclable Materials Louisiana State University Baton Rouge, LA 70813		10. Work Unit No.		
		11. Contract or Grant No. LTRC Project No. 93-1ALF		
12. Sponsoring Agency Name and Address Louisiana Transportation Research Center 4101 Gourrier Avenue Baton Rouge, LA 70808		13. Type of Report and Period Covered Interim Report		
		14. Sponsoring Agency Code Jan. 1996 - Aug. 1998		
15. Supplementary Notes Conducted in Cooperation with the US Department of Transportation, Federal Highway Administration				
16. Abstract <p>This report describes the first testing series, Phase , of the first project, Experiment 1, with the Louisiana Transportation Research Center Accelerated Loading Facility. The background to the project is described and details of the trial pavements site and the ALF are given. The objective of the first experiment is "to evaluate alternative soil-cement base courses with reduced shrinkage cracking but no loss of structural capacity", and for this, the scope of the project was established as "to compare the performance of nine base courses under accelerated loading to failure".</p> <p>The report describes in detail the methodology adopted. The evaluation criteria selected, the "as built" properties of the pavements and the loading sequences are reported. The measurement techniques for surface deformation , cracking and deflection, for "in pavement" strains and for the ambient climate are reported. Post mortem investigations are also described.</p> <p>The results for the three test pavements, lane 2, 3 and 4 of Phase I of the experiments are then discussed and interpretations in terms of layer equivalencies and pavement condition prediction are presented. The overall utilization o the ALF has a sustainable level of approximately 2, 500 cycles day and the data collection techniques are established.</p> <p>The typical crushed stone base test pavement performed in the anticipated manner to the design life. The thin crushed stone pavement with the geogrid suffered a premature localized failure, and testing had to be terminated, no conclusions to the effect of the innovative configuration can be made. The stone stabilized base test pavement performed as if it were flexible pavement with a lower stiffness than crushed stone; a layer coefficient of 0.1 is suggested for use in design. Assessment of the performance in terms of the present Serviceability Index for the crushed stone base pavement suggests a simple relationship with ESALs for use in Pavement Management Systems.</p> <p>A number of recommendations for development of the facility and for future tests have been made in this report.</p>				
17. Key Words Accelerated Pavement Testing, Accelerated Loading Facility, soil-cement base courses, crushed stone base courses, flexible pavements		18. Distribution Statement Unrestricted. This document is available through the National Technical Information Service, Springfield, VA 21161.		
19. Security Classif. (of this report)	20. Security Classif. (of this page)	21. No. of Pages 55	22. Price	

Construction and Comparison of Louisiana's Conventional and Alternative Base Courses Under Accelerated Loading Interim Report 1, Phase 1

by
J. M. Metcalf, Freeport-McMoran Professor, LSU
M. Rasoulia, Project Manager, LTRC
S. Romanoschi and Li Yongqi, Graduate Research Assistants, LSU

LTRC PROJECT NO. 93-1ALF
RESEARCH REPORT NO. 302

conducted for
LOUISIANA DEPARTMENT OF TRANSPORTATION AND DEVELOPMENT
LOUISIANA TRANSPORTATION RESEARCH CENTER
in cooperation with
U.S. Department of Transportation
FEDERAL HIGHWAY ADMINISTRATION

The contents of this report reflect the views of the authors, who are responsible for the facts and accuracy of the data presented herein. The contents do not necessarily reflect the official views or policies of the Louisiana Transportation Research Center, the Louisiana Department of Transportation and Development or the Federal Highway Administration. The report does not constitute a standard, specification, or regulation.

August 1998

ABSTRACT

This report describes the first testing series, Phase I, of the first project, Experiment 1, with the Louisiana Transportation Research Center Accelerated Loading Facility. The background to the project is described and details of the trial pavements site and the ALF are given. The objective of the first experiment is to "to evaluate alternative soil-cement base courses with reduced shrinkage cracking but no loss of structural capacity", and for this, the scope of the project was established as "to compare the performance of nine base courses under accelerated loading to failure".

The report describes in detail the methodology adopted. The evaluation criteria selected, the "as built" properties of the pavements and the loading sequences are reported. The measurement techniques for surface deformation, cracking and deflection, for "in pavement" strains and for the ambient climate are reported. Post mortem investigations are also described.

The results for the three test pavements, lane 2, 3 and 4 of Phase I of the experiments are then discussed and interpretations in terms of layer equivalencies and pavement condition prediction are presented. The overall utilization of the ALF has a sustainable level of approximately 2,500 cycles day and the data collection techniques are established.

The typical crushed stone base test pavement performed in the anticipated manner to the design life. The thin crushed stone pavement with the geogrid suffered a premature localized failure, and testing had to be terminated, no conclusions to the effect of the innovative configuration can be made. The stone stabilized base test pavement performed as if it were a flexible pavement with a lower stiffness than crushed stone; a layer coefficient of 0.1 is suggested for use in design. Assessment of the performance in terms of the Present Serviceability Index for the crushed stone base pavement suggests a simple relationship with ESALs for use in Pavement Management Systems.

A number of recommendations for development of the facility and for future tests have been made in this report.

ACKNOWLEDGMENTS

The direction and support of the Technical Advisory Committee is acknowledged. The support of the original project managers S. Cumbaa and W. Temple made this project possible. The active participation of W. King, K. Gillespie and G. Crosby, the Pavement Research Facility site manger and staff is gratefully recognized. The help of many members of the Louisiana Transportation Research Center and Louisiana Department of Transportation and Development staff was also essential and is acknowledged.

IMPLEMENTATION STATEMENT

If the conclusions and recommendations of this report are accepted, changes to the current design practice for flexible crushed stone pavements will be required. This will be accomplished by developing guidelines and specifications for use by the Louisiana Department of Transportation and Development.

TABLE OF CONTENTS

	Page
ABSTRACT	iii
ACKNOWLEDGMENTS	v
IMPLEMENTATION STATEMENT	vii
TABLE OF CONTENTS	ix
LIST OF TABLES	xi
LIST OF FIGURES	xiii
INTRODUCTION	1
Background	1
The site	2
The ALF	2
OBJECTIVE	3
SCOPE	5
METHODOLOGY	9
Evaluation criteria	9
The test pavements	9
Loading	12
Permanent surface deformation	13
Pavement surface cracking	16
Pavement surface deflections	16
In-pavement instrumentation	19
Ambient climate	23
Post mortem investigations	23
DISCUSSION	27
Profile evolution	28
Cracking evolution -- fatigue life prediction	28
Deflection and strain results	30
Layer equivalencies	30
Pavement condition prediction	31
CONCLUSIONS	33
RECOMMENDATIONS	35
REFERENCES	37

LIST OF TABLES

Table 1.	Properties of the embankment and select subgrade soils	10
Table 2.	Asphalt layer thickness	11
Table 3.	“As built” material properties-density and moisture content	11
Table 4.	Asphalt moduli	12
Table 5.	ALF loading log	13
Table 6.	Offset of the FWD geophones	17
Table 7.	Dynaflect Structural Number and subgrade moduli	20
Table 8.	Measured and predicted strains (microstrain)–lane 2	24
Table 9.	The thickness and density of asphalt cores taken after loading	25
Table 10.	Estimated and observed pavement life	27
Table 11.	Coefficients for fatigue life model	28
Table 12.	Pavement fatigue life	29
Table 13.	Estimation of layer equivalency for lane 2, 3 and 4	31

LIST OF FIGURES

Figure 1.	Plan of pavement research facility site	39
Figure 2.	The Accelerated Loading Facility (ALF)	40
Figure 3.	Embankment density contours	40
Figure 4.	Embankment Dynaflect deflection contours	41
Figure 5.	Pavement layer configuration–Phase I	41
Figure 6.	Base course gradation – Phase I– “as built”	42
Figure 7.	ALF loading history	42
Figure 8.	Transverse load distribution	43
Figure 9.	Longitudinal load distribution	43
Figure 10.	ALF profilograph	44
Figure 11.	Typical transverse profiles	44
Figure 12.	Development of rut depth	45
Figure 13.	Development of roughness	45
Figure 14.	Cracking measurement	46
Figure 15.	Crack development	46
Figure 16.	Crack patterns	47
Figure 17.	Pavement slippage failure	48
Figure 18.	Average FWD back-calculated moduli lane 2	48
Figure 19.	Strain gage configuration	49
Figure 20.	Layout of gages placed in lane 2	50
Figure 21.	Typical strain signal trace	51
Figure 22.	Discrepancy between estimated and measured strains	51
Figure 23.	Daily temperature, rainfall and river height data	52
Figure 24.	Post-mortem profile–lane 2	52
Figure 25.	Post-mortem profile–lane 3	53
Figure 26.	Post-mortem profile–lane 4	53
Figure 27.	CBR below the subgrade surface (after post mortem)	54
Figure 28.	Gradation of crushed stone base layers after loading	54
Figure 29.	Gages installed in lane 2 (after post mortem)	55
Figure 30.	PSI and ESAL’s relationship for lane 2, 3 and 4	55

INTRODUCTION

The Louisiana Pavement Research Facility (PRF) is an experimental site housing a full scale pavement testing area upon which an Australian designed Accelerated Loading Facility (ALF™) is operated. The ALF provides controlled, accelerated load testing of full-scale prototype road pavements. The Louisiana ALF is operated by the Louisiana Transportation Research Center (LTRC) for the Louisiana Department of Transportation and Development (DOTD). It is the third such device installed and operated in North America. The first two are at the Turner Fairbank Research Center [1].

This paper briefly describes the first experiment, on a series nine of test pavements, and presents the results of the first phase of the testing program: the testing of three flexible pavement configurations. The construction of the site was described by King [2].

Background

In-place, cement stabilized select soils have served as the primary base material/construction technique for the vast majority of non-interstate flexible pavements constructed in Louisiana for many years. Cement stabilized soils offer a base course which is economical and easily constructed yet provides outstanding structural characteristics. The primary attributes that detract from the performance of this base type are the potential for non-uniform in-place distribution and proper mixing of the cement and selected soils and the certainty that this type of base will undergo shrinkage cracking during the hydration process. The non-uniformity of mixing and construction provide non-uniform support (structural characteristics) to the flexible pavement which in many instances have resulted in isolated pavement failures and pavement performance variability both transversely and longitudinally along the roadway. The cracking of the cement- stabilized base courses generally results in the cracks reflecting to the pavement surface in the form of block cracking. Reflected block cracking provides avenues for moisture to infiltrate the pavement structure and has been documented to be detrimental to the rideability and performance of the pavement over a period of time.

Proposed new DOTD specifications will soon require pug mill blending of the soil cement bases in lieu of the traditional in-place stabilization process for Class 1 base course. The new requirements may increase the costs associated with construction of soil-cement base courses yet will provide for a more uniformly blended and consistent construction (base) material. It is not known at this time the affect that pug-mill mixing will have on the hydration process and the resulting shrinkage cracking associated with soil- cement base courses. It is believed that shrinkage cracking and reflective block cracking will continue to occur yet at a somewhat reduced rate or intensity.

The wisdom of incorporating a rigid base material under a flexible pavement surfacing has been questioned for many years. It has been suggested that bases which are less stiff (aggregate or relatively weaker soil cement) may offer improved performance characteristics, however

additional base thickness may be required.

Laboratory tests to compare materials are improving, but there is still a need to evaluate base designs and materials which are placed on a soil foundation using full-scale paving technologies and subjected to repeated heavy loads. The Accelerated Loading Facility device at the LTRC PRF provides an opportunity for this type of research.

The site

The facility located in Port Allen across the Mississippi River from Baton Rouge, is a 2.43 hectare (6 acre) reserve within which an embankment, 65 m x 40 m (210 x 130 ft.), has been constructed to a height of about 1.5 m (5 ft.) above natural ground to form a permanent platform for the construction of a series of test pavements (figure 1). The embankment, built of a selected silty soil (A4), raises the pavements above the level of minor flooding. A layer of select soil (A2) provides a uniform subgrade. Nine pavement lanes were built on the embankment to provide a three phase first experiment.

The ALF

The ALF is a transportable linear full-scale accelerated loading facility which imposes a rolling wheel load on a 12 m (39 ft.) test length of any test pavement (figure 2). Loading is in one direction only, at a constant speed of 17 km/h (10.4 mph) -- a cycle time of 8 seconds -- applied through a standard dual tire truck wheel capable of loads between 43 kN and 85 kN (9,750 - 18,950 lbs, 1.38 - 19.7 ESALs [Equivalent Standard (9,000 lbs) Axle Loads]). This allows the ALF to traffic a test pavement at up to 8,100 wheel passes (11,200 to 160,000 ESALS) per day.

OBJECTIVE

The objective of the accelerated loading tests in the current three-phase experiment is "to evaluate alternative soil-cement base courses with reduced shrinkage cracking but no loss of structural capacity."

This will be accomplished by determining the performance of innovative soil-cement pavements in comparison to flexible crushed stone and soil cement pavements constructed in accord with present DOTD practices.

Performance will be assessed by the measurement of transverse rutting, longitudinal profile roughness, and surface cracking of the test sections, by non-destructive testing of the pavements, and by appropriate field and laboratory testing on completion of loading.

SCOPE

The scope of the project is "to compare the performance of nine base courses under accelerated loading to failure." The performance characteristics of the historically prevalent flexible crushed stone and in-place soil cement stabilized base construction and several promising alternative base construction materials will be evaluated along with design and construction processes for pavements subjected to repeated heavy loads. A specific comparison of performance will be obtained from nine test sections representing alternative base materials and/or design methodologies under accelerated loading conditions applied at the LTRC Pavement Research Facility, using full-scale constructed test strips and the Accelerated Loading Facility device. Test strip materials selection, construction specifications and procedures, and acceptance testing will be accomplished through prior experience, engineering judgment, and laboratory testing. Performance evaluation and testing of the control and test sections will be accomplished utilizing loading records, pavement instrumentation monitoring, destructive and nondestructive testing, and visual observations.

Each alternative to in-place stabilized soil cement is specifically designed to provide a reduced level of reflective cracking.

Briefly stated, the three phases of the project are planned as follows:

- Phase I of the program will evaluate the flexible pavement "benchmark" and compare it to two innovative flexible pavements.
- Phase II will compare plant-mix stabilized soil bases.
- Phase III will compare other stabilized pavement layer configurations, including the "benchmark" pavement.

Phase I:

This phase of the research will evaluate the relative performance of three configurations of limestone bases. The control section, lane 2, is a 215 mm (8.5 in.) limestone base placed upon a geofabric, which acts as a separator to reduce infiltration of fines into the base layer. Lane 3 is 140 mm (5 in.) of crushed limestone with a high strength geogrid at the bottom of the stone layer. Lane 4 has a 100 mm (4 in.) limestone layer over a 150 mm (6 in.) limestone stabilized select soil which acts acting as a subbase. In this lane, there is no separating geo-fabric. The volume of limestone required to stabilize the select soil was determined from laboratory tests as 41 percent to give a California Bearing Ratio of approximately 36. The concept of stabilizing select soils as a subbase has been used successfully in other states but has not yet been tried in Louisiana.

The primary questions to be answered during this phase of the research are as follows:

What is the relative performance and strength of the 215 mm thick limestone base compared to the other configurations of limestone bases?

Does a high strength geogrid placed at the bottom of a limestone base layer significantly increase the strength and long term performance of limestone bases?

Are stone stabilized subbases a feasible alternative to the other limestone configurations relative to strength, performance, and cost?

What are the relative strength and performance differences between pavements constructed on bases tested during this phase as compared to the bases constructed during the other phases when subjected to accelerated loading?

Phase II:

Proposed new construction procedures will require pug-mill blending (plant mixing) of soils and cement for soil cement bases. It is believed that this construction procedure will provide an increased uniformity in the blending process and, as a result, reduce the size and intensity of base shrinkage cracks.

Another benefit of plant mixing over existing procedures is the possibility of constructing the base with a reduced cement and moisture content. It is believed that the cement content in a plant mixed soil cement base can be reduced below the levels required by current DOTD procedures for two reasons: (1) improved blending and cement distribution will reduce the chance of localized areas of low or extremely high cement content, and (2) the compressive strengths produced by current procedures have been shown to exceed 4 MPa (600 psi) after three months. It is anticipated that through proper design, a reduction in cement and water content can result in a base with adequate ultimate compressive strength (1.7 - 2 MPa [250 -300 psi]) after 30 days, which due to these reductions will experience less volumetric shrinkage.

Phase II of the research will evaluate the relative performance (strength and cracking characteristics) of the current 215 mm in-place mixed soil cement base with that of an 215 mm plant mixed soil cement base constructed utilizing the same cement and moisture content along with a 215 mm plant mixed soil cement base designed with a reduced cement and water content.

The primary questions to be answered during Phase II of the research are as follows:

Will pavements constructed on a plant mixed soil cement base have a lower level of shrinkage cracking than those constructed on an in-place stabilized soil cement base when equivalent cement contents are used?

Will pavements constructed with a reduced cement content, plant mixed soil cement base have a lower level of shrinkage cracking than those constructed on plant mixed soil cement base using standard cement contents design procedures?

What are the relative strength and performance differences between pavements constructed on bases tested during this phase, as compared to the bases tested during the other phases, when subjected to accelerated loading?

Phase III:

The research to be conducted under Phase III of this project is designed to compare the relative strength and performance of a control section and two alternative base sections. The control section, lane 8, is 215 mm of in-place stabilized soil cement. Lane 10 is a 305 mm (12 in.) reduced cement content, plant mixed, soil cement base. This experiment will explore the rationale of overcoming potential problems associated with reducing soil cement base strength by increasing its thickness as is implied in the AASHTO Pavement Design Procedure. In Louisiana, a structural design coefficient of 0.15 has traditionally been used for soil cement design with a target compressive strength of 1.7 - 2 MPa at 7 days. The modified soil cement design procedures for plant mixing will target the 1 - 1.7 MPa range at 7 days, which can be associated with a design coefficient of 0.11 (see figure 2.8 of the 1986 AASHTO Design Guide). This approach roughly equates a 215 mm base thickness at 0.15 to a 305 mm thickness at 0.11.

Lane 9 is a 150 mm thick, in-place stabilized soil cement base using the normal cement content, with a 100 mm crushed limestone, crack relief layer placed between the base and the surfacing. The concept of placing a stone crack relief interlayer between the soil cement and HMAC layers is not new but has been tried only once in Louisiana. The concept is that shrinkage, environmental, and loading induced movements of the cracked soil cement will be intercepted and be inhibited from propagating through the HMAC layers by the stone interlayer.

The primary questions to be answered by Phase III research are as follows:

Will increasing soil cement thickness overcome the potential load performance shortcomings of a lower strength base resulting from reduced in cement content?

What are the relative shrinkage cracking characteristics of the two thickness levels of reduced cement content soil cement bases as compared to the soil cement control sections?

Does a crushed stone interlayer between the soil cement base and the HMAC surfacing significantly decrease reflective cracking when the pavement sections are loaded in an accelerated manner?

What are the relative strength and performance differences between pavements constructed on high strength soil cement bases as compared to a soil cement base with less strength, yet of a greater design thickness, when subjected to accelerated loading?

What are the relative strength and performance differences of a 100 mm stone interlayer constructed between a thin soil cement base and the HMAC surfacing as compared to full thickness of extra thick soil cement sections?

What are the relative strength and performance differences between pavements constructed on bases constructed during this phase, as compared to the bases constructed during the other phases, when subjected to accelerated loading?

This report will describe the overall site preparation and experimental methodology but report only the results of Phase I of the program.

METHODOLOGY

This section of the report describes the evaluation criteria for the experiment, the test pavements for the first phase, and the procedures used to collect and analyze the performance of the lanes. The results of the investigation are summarized in each section.

Evaluation criteria

Each lane has the same extremely strong, asphalt surface, the intent being to ensure that failure would primarily be due to permanent deformation of the base, subbase, and/or subgrade. Performance was monitored and determined by measuring the development of rutting, roughness, and cracking in the trafficked area and by measurement of deflection under the Falling Weight Deflectometer (FWD) and Dynaflect equipment. The measurement and analysis procedures are described in later sections of this report.

A rut of 25 mm (1 in.) at the surface was selected as an initial failure criterion and for cracking, more than 50 percent of the loaded area having a crack density of 5 m/m² (1.5 ft/ft²) was also regarded as failure. A secondary criterion was to be any significant change in estimated pavement layer moduli.

The test pavements

Nine pavements were built for the first experiment designed to be tested in three phases. The characteristics of the embankment and select subgrade soils are given in table 1. A graphic representation of the "as built" condition of the subgrade is shown by the distribution of field density and Dynaflect deflections (figures 3 and 4).

The pavement cross sections are shown in figure 5. Phase I of the program compared three flexible crushed stone pavements and established a "control" pavement performance standard for lane 2, which is a typical DOTD design. The two other pavements in Phase I are designed for the evaluation of a thinner pavement, with a geogrid (lane 3) and a pavement with stone-stabilized soil as the sub-base (lane 4).

Construction of the pavements was completed in December, 1995 [2]. The subgrade was first placed and compacted to the required levels and then the pavements were built in sequence. Some difficulty was encountered in producing the desired asphalt mix, which was required to be so strong as to preclude failure in the binder or wearing courses since this first experiment was to compare the performance of the various base courses.

The thickness of the layers was carefully monitored to meet the specification by leveling each course up from the subgrade. Layer thicknesses were rechecked when post-mortem examinations of the pavements were conducted.

Rod-and-level elevation measurements were performed on all the test lanes before the construction of the binder course and after the construction of the wearing course. The difference in elevation for the same station represents the total thickness of the asphalt layer.

Eleven measurement stations, at 1.5 m (5 ft.) intervals, were established on the centerline of each lane to coincide with the deflection testing stations; the sixth station was at the center of the test length. The elevations were measured inside and outside the testing area in order to study the variability of the thickness of the asphalt layer.

Table 1
Properties of the embankment and select subgrade soils

		Embankment (A-4)			Select subgrade soil (A2)		
		Density	m/c	Modulus	Density	m/c	Modulus
Laboratory	Standard	1683.5	18.3	8 - 15	1749.2	15.5	
	Modified	1818.1	15.2	10 - 28			
In situ	(0.3m)	1773.2	12.2				
	(0.6m)	1371.2	35.6				
Composition	% sand	4			57		
	% silt	69			33		
	% clay	23			10		
	% organic	4					
LL		27			NP		
PI		6					
UCS(psi)		33					
CBR		10					

Asphalt layer thickness determined for the test lengths are reported in table 2. Cores were taken outside the test area and good agreement found between core length and rod and level thickness.

Table 2
Asphalt layer thickness (mm)

Method	Lane 2	Lane 3	Lane 4
Rod and Level Average (n = 11)	78.4	90.2	111.8
Standard Deviation	1.9	2.5	11.7

Table 3
"As built" material properties - density and moisture content

Lane	Layer	Density	Standard	Moisture	Standard
2	AC layer	2220	5.3		
	stone base	2213	12.1		
	select soil	1733	8.5	11	0.87
	embankment	1704	19.2	16	0.99
3	AC layer	2217	7.0		
	stone base	2200	9.8		
	select soil	1712	29.1	13	0.85
	embankment	1718	10.9	16	0.23
4	AC layer	2200	0.8		
	stone base	2197	5.3		
	stabilized stone	1933	12.8		
	select soil	1701	14.4	12	0.31
	embankment	1677	15.0	17	1.15

Ground Penetrating Radar (GPR) equipment was also used to check the thickness of the asphalt layer; the estimated thickness were much higher than those determined by rod and level, but the

standard deviation of thickness was similar. It is likely that the difference in mean thickness is attributable to the assumption of the dielectric constant.

The "as built" properties of the embankment, select soil subgrade, and crushed stone materials for the first three lanes are given in table 3. Figure 6 shows the envelope of gradations for the crushed stone base course material.

The "as laid" densities of the high-traffic, high-stability type 8 polymer modified asphalt binder and wearing courses are shown in table 3. Moduli from laboratory tests are given in table 4; those determined in situ by FWD testing are described later.

Loading

ALF performance in terms of the number of passes, transversal position, and wheel load is monitored continuously.

Loading commenced on lane 2 in February 1996, and loading of all lanes was completed by September 1996. The pattern selected was to apply the standard axle load 4,412 kg (9,750 lbs) initially, and until the design life had been attained without undue distress of the pavement. The load was then increased to 11,180 kg (12,300 lbs) until the designated failure condition was attained. During this first loading period, the usual teething troubles expected when bringing on line a major piece of equipment were experienced, but, as can be seen from figure 7, the utilization rate of the ALF is increasing towards a maximum sustainable level of 8,100 passes/day.

Table 4
Asphalt moduli

Sample	Modulus (MPa)
Laboratory mix	4189
Plant mix	4040
Binder course cores	3503
Wearing course cores	2820

The accelerated loading was applied on a single set of dual wheels (i.e. half an axle). The tire pressure was 724 kPa (105 psi). The load was always applied in the same direction (from East to West). The loading was applied over a normal transverse distribution of 0.375 m (1.25 ft.) which meant that the outer edges of the tires reached 0.55 m (1.83 ft.) from the centerline (i.e. a trafficked width of 1.1 m (3.67 ft.) as shown in figure 8. This mode of loading is called the wide

normal transverse distribution.

Figure 9 shows a typical longitudinal loading profile and reveals the dynamic load variation as the wheel first contacts the pavement. In a cycle of eight seconds, the wheel is in contact with the 12 m test pavement test length for about 3 seconds.

Loading was applied in sets of 25,000 passes (over about three days) on each lane, at which point the performance measurements were made. Loading continued until the severity of cracking and/or permanent deformation exceeded the defined failure condition or until it was judged the pavement would have been regarded as unserviceable in DOTD practice by reason of atypical distress. The ALF loading was applied in the sequence shown in table 5, and figure 7, on lanes 2, 3, and 4.

Table 5
ALF loading log

Lane	Date	ALF (1)	Passes	ESALs(2)	River stage(3)	Rainfall (4)	Air (5)
2	2/06-6/05, 1996	9.75	224172	308765	31	18.6	63.17
		14.35	50194	324404			
3	6/11-7/01, 1996	9.75	74991	103290	34.2	1.94	77.89
4	7/09-9/04, 1996	9.75	283230	396109	14.5	8.57	78.98
		14.35	41369	261368			
2	9/05-9/16, 1996	14.35	47419	306411	8.1	1.08	78.80
3	9/20-9/27, 1996	9.75	20566	28710	10.1	2.23	72.90

(1) Wheel load in kN (DOTD legal maximum kN).

(2) Estimated by 4th power law.

(3) Average height in feet; note the mean level of the pavement surface is 17 feet.

(4) Total for the test period (inches).

(5) Average daily air temperature for the test period (°F).

Permanent surface deformation

Pavement condition was monitored by measuring surface deformation (profile), cracking, and deflection. In addition, a inside pavement instrumentation was installed to measure strains in the pavement layers, pressures at the pavement/subgrade interface and, pavement temperatures.

Procedures The surface profile was determined using the ALF profilograph (figure10). This system consists of a linear variable differential transformer (LVDT) mounted on a metal carriage. A 25 mm (1 in.) diameter plastic wheel is mounted at the bottom end of the LVDT. The carriage moves transversely across the pavement on a metal frame, which travels longitudinally along the pavement test section on a set of two rails, mounted on the pavement surface outside the trafficked area.

A profile measurement session consists of collecting data on:

- eight transverse profiles, at 1.2 m (4 ft.) intervals longitudinally, from the start to the end of the test section.
- three longitudinal profiles, on the centerline (profile 1), and at 0.3 m (1 ft.) to the left and right (profiles 2 and 3).

During the transverse profile measurements the frame is locked on the rails and the carriage moves across the pavement. During the longitudinal profile measurement, the carriage is locked on the frame, and the frame-carriage assembly travels along the rails for the full length of the test section.

The principle of profile measurements is that the elevation at any point is measured by the LVDT when the wheel is placed on the point. The movement of the carriage on the metal frame and the relative movement of the frame along the rails is guided using two metal wheels connected to chains. The elevation reading is taken every inch, a total of 120 readings resulting from one transverse profile and 360 readings from a longitudinal profile. In order to determine not only the profiles but also the absolute elevation of each point, a zero reading is taken at the beginning of the testing session. This is accomplished by measuring the elevation of a reference calibration block placed outside the trafficked area.

The transverse and the longitudinal profile data are stored in separate computer files. The date of the measurements along with the number of load repetitions applied to the tested section are recorded in the file header.

Transverse rut depth is defined as the maximum depth under a 1.2 m (4 ft.) straight edge. One transverse profile is calculated by placing a straight line, simulating the 1.2 m (4 ft.) beam, at the initial point of the profile. The line connects two points at 1.2 m apart on the horizontal from each other. Between these two points, 47 vertical distances between the straight line and the measured pavement profile are calculated, the maximum positive value being the rut depth for the initial point. Next, the line is placed into a new position, starting with the second point of the transverse profile and a rut depth is calculated again for this new position. The line is successively placed on the transverse profile, and rut depth values are computed until the last point of the transverse profile is reached. A total of 72 rut depth values result from these calculations. The maximum of these 72 values is defined as the rut depth for the transverse profile (figure 11). A QuatroPro spreadsheet macro was created for this calculation.

The data measured on the central longitudinal profile only is used for the determination of the surface roughness; the Slope Variance (SV) and the International Roughness Index (IRI) are computed.

Since the area where the ALF machine tire first contacts the pavement is subjected to higher loading than the rest of the test areas, and larger depressions develop there, the elevation readings on the first 1.5 m (60 in.) were not used for the IRI and SV computations. The same procedure was kept for test lane 4, even though the depression was not so pronounced.

The slope variance measure (SV) of pavement roughness was developed in association with the CHLOE profilometer at the AASHO Road Test, where the wheelbase of the slope variance determination was 230 mm (9 in.). Since CHLOE profilometers are not used now for routine roughness measurements, a relation, operating on measured profile points is used in this study Shahin [3]. The elevation readings are taken at one inch intervals, which are much smaller than usually used in routine pavement profile measurements. The surface profile now containing 300 elevations is further modified. New profiles are created from the measured profile by keeping the readings at 50 mm to 300 mm (2, 4, 6, 8, 10 and 12 in.). For each of the six new profiles, the Slope Variation (SV2-SV12) and International Roughness Indexes (IRI2-IRI12) were calculated; as there was little difference between the results, data for the 250 mm (10 in.) base is reported.

The Slope Variance (SV) was computed as follows :

$$SV = \left(\sum_{i=1}^n X_i^2 - \left(\sum_{i=1}^n X_i \right)^2 / n \right) / (n - 1) \quad (1)$$

where :
SV - slope variance
 X_i - the i^{th} slope measurement
n - the total number of measurements.

The i^{th} slope was calculated as $100 * (H_{i+1} - H_i) / p$, where H_i is the elevation in point i and p is the distance between two adjacent points (the step of measurement).

The International Roughness Index (IRI) was calculated following the procedure presented by Shahin [3].

$$IRI = 1000 * \left[\sum_{i=1}^n |C_{i,3} - C_{i,1}| \right] / n \quad (2)$$

where :

$$C_{i+1,j} = a_{1,j} * C_{i,1} + a_{2,j} * C_{i,2} + a_{3,j} * C_{i,3} + a_{4,j} * C_{i,4} + a_{5,j} * T_i, \quad j = 1 \text{ to } 4 \quad (3)$$

$$T_i = (H_{i+1} - H_i) / p$$

The coefficients depend on the distance between two adjacent points (step of measurement). These values are presented by Shahin [3]. The values of $C_{i,j}$ terms for the starting point on the profile are:

$$C_{0,1} = C_{0,3} = (H_n - H_0) / (n * p), \text{ and } C_{0,2} = C_{0,4} = 0 \quad (4)$$

The IRI values are expressed in m/km. The IRI expressed in in/mile can be obtained by multiplying the result of the calculations by 63.36.

Results The development of transverse permanent deformation (rutting) is shown in figure 12 for all three lanes together. The evolution of roughness is shown in figure 13 for the three lanes combined. The rut depth and roughness data are contained in computer files, RUTDEPTH.

Pavement surface cracking

Procedures Surface cracking was recorded by sketching in relation to a coordinate grid 1.8 by 2.4 m (6 x 8 ft.) with cross wires at 300 mm (1 ft.) centers. The crack patterns were drawn by hand on graph papers and a "PlanWheel" distance measuring device was used to measure the drawn length of the crack. Only the cracks wider than 0.1 mm were recorded. The measurement procedure is shown in figure 14.

Results Cracking occurred only in areas that were subjected to ALF repeated loading. The asphalt pavement surface showed individual transverse cracks first and, later, longitudinal cracks appeared and progressed as the transverse cracks grew longer and wider. These transverse and longitudinal cracks gradually developed into alligator cracks with the increase in ALF loading passes.

The development of cracking in the three lanes is shown in figure 15. Figure 16 shows the crack patterns of the three lanes after the test finished.

Cracking in lane 3 took an exceptional form, where a large area of slippage failure of the top asphalt layer occurred in the area where the wheel loading began and where two "in-pavement" deflection transducers were installed (figure 17). A severe circular large open crack developed at which it was easy to lift by hand the top, wearing course, layer of asphalt from the binder course over a longitudinal distance of two m (6.2 ft.). Cracking in lane 4 was similar to lane 2 until partial slippage failure again happened at the start of loading.

Pavement surface deflections

Procedures Pavement surface deflections were measured by the Dynaflect and KUAB Falling Weight Deflectometer (FWD) methods. The primary objective of FWD deflection tests on the ALF test sections was to study the change in dynamic deflection and back calculated moduli of the pavement materials, with the number of passes. The testing schedule followed the operating intervals of the ALF loading, as determined by the performance of the pavements.

The FWD used for determining the dynamic deflections at the PRF project is a KUAB - FWD Model 2m-14, FW874, which is a trailer mounted device. Several versions of this equipment exist. The model purchased by LTRC has a loading range from 7 to 150 kN (1574 to 33,000 lbs). The impulse force is created by means of a two-mass assembly in which the falling weight

is dropped onto a second weight/buffer combination. This system has good reproducibility of the load pulse (time and shape). Also, it allows an internal calibration of the load cell. The loading plate is 300 mm (12 in.) in diameter, segmented in four quadrants that can move independently. In this way, a more uniform distribution of the load is developed for testing on uneven road surfaces. A rigid plate 450 mm (18 in.) diameter can replace the smaller one to allow testing on base or subbase layers.

Before beginning the test session, more than 20 drops are performed outside the testing area, in order to warm up the FWD equipment, as recommended by SHRP protocol [4]. At the beginning and the end of each testing session, the temperatures of the air and the pavement surface are collected, using an electronic thermometer and a infrared digital thermometer. These values, along with the time of testing are recorded in the header of the FWD output data file.

The measurements are performed on the centerline of the loading path of each pavement test section, at 11 stations disposed at intervals of 1.5 m (5 ft.) along the centerline. The stations are labeled as a function of position along the centerline, from 15.2 to 30.4 m (50 to 100 ft.), the middle of the test section being at 22.9 m (75 ft.).

For each station, after one settling drop at load level 1 - 13.3 kN (3,000 lbs) for which the deflection values is not recorded, four sets of five recorded drops are performed, corresponding to the four load levels, 13.3, 26.7, 40 and 62.3 kN (3,000, 6,000, 9,000 and 14,000 lbs). The deflections are measured with the geophones position similar to the configuration recommended in the SHRP Manual [4], except for the last geophone which is closer to the loading plate (table 6). Among the total twenty deflection bowls recorded for each station, only the two last bowls corresponding to the 40 kN (9,000 lbs) load level are considered in the back-calculation analysis. Deflection bowls for both FWD and Dynaflect test are available on disk (file name DEFLECT).

Table 6
Offset of the FWD geophones

Geophone number		0	1	2	3	4	5	6
Offset	(in)	0	8	12	18	24	36	48 (60 after SHRP)
	(mm)	0	200	300	450	600	900	1200 (1500)

Dynaflect deflection measurements were performed after a short time interval, at the same locations as the FWD measurements, in order to avoid important changes in asphalt temperatures. The Dynaflect equipment is a fixed-frequency device that generates a light load by two counter-eccentric rotating masses at a frequency of 8 Hz. The peak dynamic load is around 4.4 kN (1,000 lbs), distributed by two steel wheels. Five geophones are mounted on a beam at 200 mm (12 in.) intervals, the first of them being positioned between the steel wheels.

A remote control and readout panel placed in the vehicle allows the operator to conduct the test and manually record the data.

Back-calculation of the resilient modulus of the pavement layers is done using the MODULUS 4.0 back-calculation program [5], following the procedure described by Roberts [6]. The back-calculation is performed for two deflection bowls for each station (each taken from the last two drops at the 40 kN (9,000 lbs) load level), considering that a good contact of the plate and the pavement surface was developed for these drops.

The embankment soil and the existing subgrade are modeled as a semi-infinite layer, even for the cases when the A4 selected soil is the subbase material. This assumption is reasonable because the two soil types have similar moduli and the back-calculation cannot detect such a small difference. Also, the embankment is thick enough, 1.5 m (5 ft.), to be considered as part of the subgrade.

The assigned thicknesses of the pavement base layers are the design thicknesses. For the asphalt course, the design thickness of 89 mm (3.5 in.) was adopted for the test lanes. The MODULUS program, like any other back-calculation program, allows the operator to assign only one value for the thicknesses of a layer for the entire road sector, not individual values for each station. The analysis can be done separately for each station, each with a different thickness, but the procedure is cumbersome. Therefore, the asphalt thicknesses from rod-and level investigations can not be conveniently used here.

Typical limits for the moduli of pavement materials, recommended by Roberts and the SHRP procedure, were used as moduli limits in the back-calculation process [6] [7]. The moduli limits are different for each deflection data file and are assigned in such a way to allow free iterations, i.e. the material moduli value, being within the interval, will never exceed the limits.

The back calculated asphalt moduli values reported on disk (file name BACKMODULI) correspond to the standard temperature of 20°C (68°F). The temperature correction equation recommended by Ullitz [8] is used.

$$E_{st} / E_{field} = 1 / \{3.319 - 1.751 * \log[(t_p - 32) / 1.8]\}, \quad (5)$$

where E_{sd} and E_{field} are the moduli at the standard temperature (70°F) and at the field temperature t_p . This relation is valid only for temperatures greater than 35°F. For temperatures approaching 32°F, the modular ratio approaches zero.

Since no data on the mid-depth asphalt temperature at the time of testing are available, this was estimated using the relation recommended by Jameson [9]. He proposed a method for predicting the asphalt temperature T_{ac} when only the surface temperature T_s and the mean air temperature T_{ma} of the month of deflection measurements are available:

$$T_{ac} = -2.6 + 0.842 * (T_s + T_{ma}) + 1.31 * \log(AC_t) - 0.165 * (T_s + T_{ma}) * \log(AC_t), \quad (6)$$

where all temperatures are expressed in °C, the asphalt layer thickness (A_c) being measured in millimeters.

The deflection values are available on computer file DEFLECT. Due to several electronic malfunctions of the FWD equipment, tests were performed on the test lane 2 for a total of 12 testing sessions, and for only four testing sessions on lane 4. No data were obtained in lane 3.

Results The results of the back-calculated modulus from FWD deflection data deflection for lane 2 are shown in figure 18.

The back-calculated moduli are not always in the expected range. In many cases the moduli values are higher than 1,000,000 psi which is much higher than the values recommended by the AASHTO Design Guide [10] or those from laboratory testing. Newcomb [11] mentioned that Back-calculated moduli can differ from laboratory test results. Since the ratio of the two being between 0.8 and 4.0, it is not unusual to obtain high values and high variation in the same road section, especially in the case of thin asphalt [12]. Vogelsang [13] reported a difference in central deflection of 50 percent within 1.5 m (5 ft.) for a similar accelerated test on a flexible pavement. The SHRP [7] back-calculation procedure recommends 3,000,000 psi as the upper limit of the moduli for asphalt concrete, and Witzak [14] reported similar values for data assembled from 56 road sections.

The values of the Dynaflect deflections are also available as computer file DYNAFLEC. The data is used to determine the subgrade modulus and the structural number (SN) of the pavements. The procedure recommended by Temple [15] was used to calculate the subgrade moduli and the Structural Numbers which are reported in table 7.

The subgrade moduli estimated from Dynaflect deflection bowls are generally higher than those obtained from FWD deflection data. The Structural Number (SN) is computed after the subgrade modulus and since the SN values so derived are much lower than expected (and in some instances even negative) it must be concluded that the procedure recommended by Temple [15] overestimates the subgrade moduli for this pavement configuration. Therefore, subgrade moduli values from FWD deflections were adopted for theoretical strain computations in this report.

In-pavement instrumentation

All the pavements are instrumented to measure strain at various layer interfaces and pressure at the subbase/subgrade interface. A number of lined bores allow monitoring of moisture content by down-the-hole meters. Ambient climate is recorded and "in pavement" temperatures are measured.

Instrumentation procedures Strain and pressure gages are installed in order to obtain valuable information on the mechanical behavior of the pavement structure. A total number of 36 strain gauges were used for lane 2, 36 for test lane 3, and 44 for test lane 4. Pressure gages were installed at the base/subbase interface.

Table 7
Dynaflect structural number and subgrade modulus

Lane	Passes	ESALs	Structural Number		Subgrade Modulus	
			Average	Standard Deviation	Average (KPa / psi)	Standard Deviation (KPa / psi)
2	0	0	1.136	0.123	29.99/4350	0.70/102
2	25	34	0.764	0.172	32.84/4763	1.07/155
2	50	69	0.800	0.222	32.72/4745	0.90/130
2	75	103	0.711	0.251	29.41/4266	0.92/133
2	144	198	0.409	0.334	41.93/6081	1.97/285
2	214	295	0.745	0.192	36.54/5300	2.18/316
2	243	468	0.455	0.162	37.48/5436	4.11/596
2	271	645	0.867	0.141	28.66/4157	1.80/261
2	297	811	0.455	0.162	38.00/5511	3.02/438
2	322	990	0.967	0.226	40.38/5856	2.39/347
3	0	0	0.755	0.108	34.92/5064	1.42/206
3	1	1	0.222	0.181	26.50/3844	1.66/241
3	25	34	0.267	0.287	31.41/4556	3.21/465
3	50	69	0.144	0.263	31.79/4611	2.65/384
4	0	0	0.791	0.156	34.54/5009	1.45/211
4	1	1	0.267	0.125	28.66/4156	1.18/171
4	59	81	0.111	0.159	40.14/5822	5.12/742
4	84	116	0.811	0.256	42.90/6222	3.45/501
4	109	150	0.811	0.269	38.31/5556	4.56/662
4	134	185	0.389	0.296	38.46/5578	5.19/752
4	184	253	0.500	0.313	44.97/6522	3.12/452
4	210	289	0.356	0.241	37.69/5467	3.56/516
4	258	355	0.433	0.226	34.09/4944	2.80/406
4	325	788	0.244	0.271	41.60/6033	

The strain gages were of an innovative design using 13 mm (0.5 in.) gage length (MicroMeasurement) and 25 mm (1 in.) gage length on a 100 mm (4 in.) substrate (Kiowa) resistance gages placed between two layers of bituminized tape (figure 19). Tensile gages were placed longitudinally and transversely to the direction of loading. Figure 20 shows the layout of gages placed in lane 2, a typical installation. All gages were connected to a data acquisition system linked to a PC on site.

The voltage signal is measured when the wheel passes over a gage location and is recorded by the data acquisition system. Information on the data acquisition system, the gage installation plan which gives the identification and the position of the gages in the pavement structure, is contained in the construction and instrumentation report [2].

The voltage signal collection was performed with the ALF machine running at the loading speed (17 km/h -- one pass every eight seconds). Slow speed strain responses were measured with the ALF wheel pushed by hand. Due to this, the frequency and the number of passes recorded in one measurement session varied. A low data sampling frequency (30-40 Hz) was applied when the ALF wheel was pushed by hand. Multiple passes at a high data sampling frequency (100 Hz) were recorded when the ALF machine ran at the normal speed.

Files containing the strain information, resulting from the data acquisition process, are of the "comma delimited" type. The strain data file contains information on the day of testing, the number of wheel passes, the frequency of data sampling, and sets of voltage and sampling time for each gage.

To analyze the data, the voltage signal was first displayed graphically, and the strain data calculated only when the signal has the expected characteristic shape (figure 21). Otherwise, the signal cannot be interpreted. A similar signal for a gauge measuring negative strain (compression) should show the peak downwards.

The strain data file is then processed using a QuattroPro macro. For each pass of the ALF wheel above the gauges and for each strain gauge, the macro will calculate three voltage values: the average voltage, the maximum voltage and the minimum voltage (figure 21). It was considered that the average voltage value is the voltage measured when no dynamic strain is developing in the pavement structure. Therefore, for each pass, the difference between the maximum voltage and the average voltage, and the difference between the average voltage and the minimum voltage are indicators of the dynamic strain. These differences were next used in the strain calculation. Since, in most cases, the strain data was collected for more than one wheel pass, the means and the coefficients of variation of the two voltage differences is computed.

When only one wheel pass is recorded, the coefficients of variation are zero, since only one difference is calculated for the maximum and one for the minimum voltage. The coefficients of variation are useful since the strain values are not exactly the same for two consecutive passes of the loading wheel, and the voltage signal is affected by electrical noise.

The mean values of the two differences (U^+ and U^-) are then used to compute the strain values,

using the formula :

$$g = \frac{4,000 * U}{U_0 * F} \quad (7)$$

where :

- g - the strain (microstrain)
- F - strain factor (2.085 for MicroMeasurement gauges and 2.00 for Kiowa gauges)
- U - the voltage difference (millivolts)
- U_0 - the excitation voltage of the Wheatstone bridge (volts). An excitation voltage of ten volts was applied to each Wheatstone bridge containing the strain gauges.

Note that there is a small constant term in the calculation of strain but of negligible size. For all the gauges, two strain values (g^+ and g^-) corresponding to the two differences, and the coefficients of variation of these strains (same as the coefficient of variation of the differences) are stored in separate files.

Next, the measured strain is selected between the two calculated values (g^+ and g^-) function of the shape of the signal that has been previously visualized graphically. A signal having an upper peak indicates that the measured strain is positive (tension) and the g^+ value is selected. For a signal having downward peak, the g^- value is considered as the measured strain.

The pressure cells were of Kulite type. The cell voltage data was recorded in the same file as the strain data. The voltage differences (U) are computed using the same procedure as for the strain gauges. The conversion from voltage to stress is obtained by using the following formula :

$$F = (a + b * U) \quad (8)$$

where: F - measured stress (MPa), U - output voltage difference (Volts), and a , b - regression constants.

The regression constants were acquired from data obtained during the pressure cell calibration process, performed in LTRC laboratory. The calibration consisted of measuring the output voltage of the pressure cells when placed in a triaxial chamber and subjected to known confining pressure levels. Air was used as the confining fluid.

The theoretical values of the strains at the same position as the gauges were calculated using the linear elastic model, CIRCLY. The thickness (h) and the Poisson's ratio (n) for each layer of the structure were defined as follows :

- AC surface layer	$h = 89 \text{ mm (3.5 in)}$	$n = 0.35$
- crushed stone base layer	$h = 216 \text{ mm (8.5 in)}$	$n = 0.40$
- subgrade and capping layer (A4 soil)	$h = 50 \text{ mm (2 in)}$	$n = 0.45$

The modulus values of pavement materials were taken from the FWD moduli back-calculation data at the appropriate number of load passes.

Strain measurement results Calculated strain levels indicate that the strains should be measurable by the equipment installed and several apparently reasonable strain traces were obtained from lane 2. Traces from lanes 3 and 4 so far have proved impossible to analyze due, apparently, to low strain levels such that no signal measured had a clear peak voltage record.

It is suspected that this results from high electrical noise interference, damage due to the high moisture in the foundation layers, in many cases reaching saturation levels, or to very low strain transference between the gages and the pavement layers. Excavation of the gages at the post mortem supports the third hypothesis.

Signals with clear peaks were obtained for only 15 of the 36 the gauges mounted in test section 2. The strain values computed from the voltage data are reported in table 8 which contains information on the type and position of each gauge and the strain recorded relative to the number of passes the pavement structure had carried. Figure 22 illustrates the discrepancy between theoretical estimates of strain and measured strain for the critical bottom of asphalt location. There is an order of magnitude difference in these data.

No acceptable results were obtained from the pressure cells mounted in the three pavements.

Ambient climate

Procedures Ambient climatic conditions were recorded from a full weather station installed at the site to measure air temperature, wind speed and precipitation. Pavement surface temperature was measured by infra red thermometer initially and, later, in pavement temperatures, were measured by thermocouples placed at the layer interfaces.

Results The daily temperature, rainfall and river height data are shown in figure 23 for the test period, and also summarized in table 5. The data in detail are available in computer file CLIMATE.

Post mortem investigations

After completion of loading of all three lanes, trenches were cut through the asphalt layers and the crushed stone layers were excavated to the subgrade. Cone penetrometer tests were performed to estimate subgrade strengths and nuclear density gage readings were taken on the stone materials. Samples were taken to determine the in situ gradations, moisture contents and plasticities.

Layer thicknesses were measured and the profile for each lane is given in figure 24, 25, 26. There is some indication that the asphalt layer is thinner after trafficking.

The penetrometer results showed CBR values of about ten, but also indicated the presence of a

Table 8
Measured and predicted strains (microstrain) -- lane 2

GAGE	Sign	Passes(x 1,000)							
		100	125	150	175	180	217	225	250
In Asphalt - Transverse									
AT1-1		55.48	26.34	97.13					
DT2-1					25.48		17.64		
FWD(1)		-26.1	-63.1	-79.1			-87.8	-154	-131.5
In Asphalt - Longitudinal									
AT1-3		24.77	19.65	33.03					
DT2-3					28.92		17.28		
DT2-4						30.75		46.86	
FWD		-55	-129	-156			-172	-245	-218.4
Bottom of Asphalt - Transverse									
BT1-1		54.07	29.35				39.94		37.52
BT2-1				112.4					
BT3-2		24.53	41.49	26.57		29.89	30.06	27.67	
BT3-2						59.14	38.43	34.63	33.23
ET2-1		-43.56	-109.5		27.03		22.44		
FWD		15.8	-157	-256			-261	-291	-160.7
Bottom of Asphalt - Longitudinal									
BT1-3		38.29	27.83	99.22					
BT3-3		22.68	60.01	41.0		62.95	59.52		
BT3-4						65.21	48.01		
ET2-4							23.49		
FWD		361	620	656			726	1037	1072
Bottom of Stone Base									
CT3-3							378.9		
FWD		560	1009	1072			1214	1750	1789

(1) FWD strain predicted from back-calculated moduli.

(2) “-” indicates compressive strains.

weaker layer with CBR 5 at about 0.3 to 0.6 m (1 - 2 ft.) below the subgrade surface. The results did not define the select soil/ embankment soil interface (figure 27).

This soft layer and the evidence of water penetration at the asphalt layer interfaces, observed in the post mortem trenches, emphasizes the difficulties in interpreting the effects of the high rainfall and high ground water tables experienced. The excavation of all lanes showed evidence of separation between the asphalt layers and the asphalt and base. Moisture was present at the interface between the asphalt wearing and binder courses which probably resulted in the localized failure in 3 and would affect stress distributions in all lanes.

Grading of the crushed stone after loading indicated little change in gradation, suggesting no breakdown of particles occurred under traffic. The results of these tests are given figure 28.

Cores were taken in trafficked areas to determine in situ density of the asphalt and to determine the layer thickness at the points where FWD deflection testing was carried out. The results of these are given in table 9.

Finally, the strain gages installed in lane 2 were carefully excavated. Figure 29 shows the condition of the gages. It is evident that the installation procedures were satisfactory in that there was no apparent damage to the gages, however, the bond between the gages and the asphalt layers depended entirely upon the bitumen tape film. This film is viscoelastic and strains freely under a small load. It is thus unlikely that it could transmit small transient strains in the asphalt to the gages except perhaps where some stone-gage contact occurred. This may have contributed to the difficulties in measuring strain.

Table 9
The thickness and density of asphalt cores taken after loading

Lane	Thickness (mm)	Density(kg/m ²)
2	92	2234
3	107	2219
4	117	2212

DISCUSSION

The response of lane 2 to loading was typical of a flexible pavement; deflection, deformation, roughness and cracking all increased with the number of load repetitions, and at an increasing rate when the wheel load was increased. Failure was assessed at 880,000 ESALs when rutting exceeded 25 mm and cracking was more than 2.5 m/m². In DOTD practice, the pavement would have been rehabilitated when rut depth exceeded 19 mm. The modulus, back calculated from FWD data, decreased with loading.

The response of lane 3 was unexpected with a premature localized failure, the development of a large U-shaped crack occurred at the most heavily loaded section of the test lane. This crack extended quickly to the point at which it was considered a road in service would have been patched. In opening the pavement to lay the patch, it was seen that water was present at the interface between the asphalt wearing and binder courses which could easily be separated. Trafficking was stopped at this stage, after 146,000 ESALs, although apart from the localized surface failure, deformations were not extreme. Due to the extremely high watertable evident at this stage (figure 23) it was decided to cease loading the lane 3, and to begin testing lane 4.

This lane performed, and failed, in a very similar manner to lane 2, but with a shorter life (674,000 ESALs). Cracking developed more rapidly than in lane 2, but rut development was slower. Again loading was stopped when it was considered that, in practice, the pavement would have been rehabilitated.

Initial estimates of pavement life, based on the Structural Number, as assessed by the DOTD procedure, are given in table 11, together with actual performance from the results above. The design life is the ESALs estimated by the usual DOTD (AASHTO) procedure, using typical layer coefficients and the designed layer thicknesses with an assumed subgrade CBR of ten. The rutting life is the observed or extrapolated ESALs to a 25 mm rut depth. The cracking life is the observed or extrapolated ESALs to the criteria proposed by Jameson [16]. The Pavement Serviceability Index (PSI) life is the ESALs estimated to reach a terminal PSI of 2.5 to accord with the design procedure.

Table 10
Estimated and Observed life (ESALs x 1000)

Lane	Design life	Rutting life	Cracking life	PSI life (2)
2	863	840	973	1,003
3	481	-	(146)	(18)
4	648	674(1)	657	650

(1) extrapolated.

(2) has equated 5.5

Profile evolution

The development of rutting and roughness followed a typical pattern, increasing with number of ESALs (figures 12 and 13). No rutting model has been applied but the related project by Roberts will in part address this.

Cracking evolution – fatigue life prediction

A pavement fatigue prediction model, based on data from a full-scale accelerated pavement test, using an ALF, was developed by Jameson et al [16]. It is given as :

$$\text{Log}(N) = a + b \text{ Log } (\mu\epsilon) + 1.8 \text{ Log } (E) \quad (9)$$

Where N - number of load repetitions to a certain cracking severity (5.0 m/m²)

E - initial asphalt layer modulus (MPa)

$\mu\epsilon$ - initial horizontal asphalt strain at the bottom of asphalt layer, and

a, b - constants, see table 11.

Table 11
Coefficients for fatigue life model

Cracked Area (%)	a	b
10	22.800	-4.603
50	24.467	-5.119
90	25.322	-5.319

The Jameson model was used to examine the result of these Phase I tests, because the pavement configurations are similar.

The FWD deflection bowls, measured before ALF loading for each of three lanes, were used to determine the initial asphalt layer modulus and tensile strain.

Because the asphalt layer moduli are sensitive to loading duration time, the effect of different loading times of 35 and 144 ms, corresponding to the FWD and ALF load duration respectively, on the modulus value was considered. The back-calculated moduli of asphalt layer from FWD deflections is converted to the corresponding values under ALF loading by using the following equation to take account of temperature variance at the time of testing.

$$\frac{E_{ALF}}{E_{FWD}} = 0.91 - 0.011 T \quad (10)$$

where: E_{ALF} - asphalt layer modulus under ALF loading (MPa)
 E_{FWD} - asphalt layer modulus under FWD loading (MPa), and
 T - asphalt pavement temperature.

Although the moduli of aggregate base and subgrade are believed to be sensitive to loading time and magnitude, the back-calculated moduli of these two layers were not converted because there is no existing equation relating the moduli at FWD and ALF loading.

The converted moduli of the asphalt layer and back-calculated moduli of the base and subgrade were used as input into CIRCLY to calculate the horizontal tensile strain at the bottom of the asphalt layer under ALF loading (9.75 kip). The resulting strain and converted modulus of the asphalt layer then were used with equation (9) to estimate the pavement fatigue life. The results are given in table 13. Jameson's model reasonably predicted the fatigue life for lane 4, but not for lane 2 or 3. It should be noted that the back-calculated asphalt layer moduli of three lanes are quite different. In fact, the asphalt layer moduli, as well as other layer moduli from back-calculation procedure, are not necessarily material parameters but complex indicators of the whole pavement structural bearing capability.

The observed pavement fatigue life of lane 2 and 4 was determined from the recorded crack data according to Jameson's criterion, which defines the pavement fatigue failure as 50 percent loaded area having a crack rate of 5 m/m² [16]. For lane 4, the cracks, caused by pavement slippage failure, were not counted when the crack rate was calculated (figure 17). Lane 3 had not reached the failure criterion of 5 m/m² during the loading period but loading was stopped because of the local failure described above.

Table 12
Pavement fatigue life

Lane	Modulus (MPa)				Strain 10 ⁻⁶	Fatigue life (x1,000)	
						Predicted	Observed
	Asphalt layer	Base	Subbase	Subgrade		ESALs	ESALs
2	2397	118		29	658	12	973
3	3320	98		37	621	9	132
4	5215	69	151	42	441	772	657

It is noted, from figure 15, that the crack deterioration rate of lane 3 was greater than that of lane 2 and 4 during first period of loading. Much higher Dynaflect deflections were also observed on lane 3 than on lane 2 and 4 during loading, because a higher watertable existed when lane 3 was loaded (figure 23). The initial crack on lane 3 was observed at 42,400 ESALS. At 114,000

ESALS, partial slippage failure of the top lift of asphalt occurred at the start end of loading, where an LVDT transducer was located in pavement. Similar slippage failure was also observed at 425,190 ESALs on lane 4 at almost the same position, and the pavement layers could easily be separated. There are two possible reasons for this type of failure. First, water entered the interface between the asphalt layers and between the asphalt and the base course, through the LVDT hole and through cracks and extended over the interface under ALF loading. Second, ALF exerts a horizontal force on the pavement surface where the wheel first impacts the pavement.

Comparing lane 2 and 4, at the same load passes, we can conclude that lane 4 had more severe cracking than lane 2. It should be noted that during ALF loading, the moisture condition of lane 2 was worse than lane 4, while the temperature of lane 4 (79 °F) are bigger than that of lane 2 (65 °F).

Deflection and strain results

The FWD derived moduli, available only for lane 2, were usually higher for asphalt and lower for other layers than typical values in the literature for similar materials. The determination of the Structural Number from Dynaflect deflection data, using the current DOTD procedure, gave results much less than normally expected.

The very limited strain data show the measured strains are generally much smaller than theoretical estimates predicted by the linear elastic model. Also, important differences between the strains measured by different gauges were encountered, even within groups of gauges placed at the same position in the pavement structure. This is attributed primarily to inefficient bonding between the strain gage assembly and pavement layers (figure 29).

Among the different causes for these large differences are the inaccurate estimation of asphalt layer thickness, post mortem measured thicknesses were 12-37 mm (0.5 - 1.5 in.) more than the design thickness. This significantly affects the estimated strains. Thickness differences also affect the neutral axis of the layers and may result in a change in sign of the strain for gages near the zero strain plane.

Other causes for poor agreement include differences in the actual and estimated ALF wheel load and placement of the load in relation to gage position. The modulus values used in strain estimation also vary and a wide range of moduli were apparent.

Layer equivalencies

The layer coefficients (a_i) for the AASHTO design procedure may be estimated from the structural number of a pavement provided information on the component materials and layers is available or may reasonably be assumed. Using the rut depth, cracking and slope variance data collected for the test lanes, the PSI may be estimated against life in ESALs. Given a terminal PSI value the terminal SN can be estimated and thus layer coefficients assigned. Similarly SN estimates can be based on the moduli determined from FWD data assuming, or knowing layer

thicknesses.

An alternative approach, which is considered valid for comparative purposes, is to compare the life of the different pavements where a direct comparison of pavement layers and materials may be established. This is done for lanes 2, 3 and 4 in table 14 assuming that the initial PSI is five and the terminal PSI is 2.5, and the layer thicknesses are as designed and the layer coefficients are typical Louisiana values for the materials. The results indicate that where a value of the layer coefficient for the crushed stone base is 0.14, then a comparable coefficient for the stabilized stone layer would be 0.10. In relative terms this means that, for the same performance, the thickness of stabilized stone required would be some 30-40 percent greater.

Table 13
Estimation of layer equivalency for lane 2, 3, and 4

Lane	Actual ESALs (x 1,000)	Design ESALs (x 1,000)	a1	d1	a2	d2	a3	d3	a4	d4	Subgrade CBR
2	880	863	0.44	3.5	0.14	8.5	0.06	3.5			10
3	146	481	0.44	3.5	0.14	5.5	0.06	6.5			10
4	674	648	0.44	3.5	0.14	4	0.10	6	0.06	2	10

Pavement Condition Prediction

The relations between PSI and ESALs estimated from the profile and cracking data for the three test lanes (figure 30) can be expressed for full depth crushed stone pavement by the following linear regression model:

$$\text{lane 2: } \text{PSI} = 5 - 0.0025 (\text{ESAL} = s \times 10^{-3}) \quad r^2 = 0.91, n = 13 \quad (11)$$

$$\text{lane 3: } \text{PSI} = 5 - 0.0154 (\text{ESAL} = s \times 10^{-3}) \quad r^2 = 0.91, n = 5 \quad (12)$$

$$\text{lane 4: } \text{PSI} = 5 - 0.0049 (\text{ESAL} = s \times 10^{-3}) \quad r^2 = 0.42, n = 7 \quad (13)$$

Equation (11) could be adopted as an interim means of predicting pavement performance for PMS modeling as it has a reasonable correlation coefficient and sample size (13 observations).

CONCLUSIONS

- (1) The establishment of the Pavement Research Facility has been successfully accomplished and the operation of ALF has begun.

Mechanical utilization has reached a reasonable average level of around 60 percent. There is a significant dynamic impact effect at the start of every loading cycle. This causes results from the first 2-4 m of the test pavement to be incompatible with the remainder of the test length. Efforts should continue to reduce this effect.

The instrumentation technologies are working well with the exception of the strain gages and pressure cells. Some limited exploration of alternative gaging techniques and data acquisition is warranted.

- (2) Performance of the first and third test lanes (lane 2, 4) followed the anticipated pattern, rut depth gradually increased, as did roughness, and cracking initiated after some trafficking.

The life of lane 2 was in reasonable agreement with that predicted by DOTD procedures, as estimated using the AASHTO design procedure.

Using the same design approach, the performance of lane 4 can be back-analyzed to suggest a layer coefficient for the stone stabilized soil of 0.10, which is a creditable value but, it must be emphasized, based on limited evidence. Estimating the Present Serviceability Index (PSI) from the roughness, cracking, and rutting results gave a reasonable relationship for lanes 2 and 4 which could be applied in Pavement Management systems models.

- (3) Performance of the second pavement, lane 3, was unexpected and resulted in a localized failure. Post mortem examination suggests that the wearing course of the asphalt separated from the binder course leading to slippage and cracking where the ALF wheel load is first applied to the pavement surface. At this point the dynamic vertical load is at maximum, and there is a real possibility of surface shear loading as the wheel speed may change to balance with the bogie speed at first contact.

It is not possible to reach any conclusion as to the effect of the geogrid reinforced base layer.

- (4) It is clear that the performance overall of ALF, the instrumentation, and the pavements was greatly affected by the high rainfall and high ground water tables encountered. The machine difficulties have effectively been solved but provision for drainage of the pavements and enhanced moisture movement measurement should be included in future experiments.

The primary questions answered during this Phase of the research are as follows:

What is the relative performance and strength of the 215 mm thick limestone base compared to

the other configurations of limestone bases?

The 215 mm crushed limestone base, typical of current practice, performed in accord with expectations and better than the other configurations tested.

Does a high strength geogrid placed at the bottom of a limestone base layer significantly increase the strength and long term performance of limestone bases?

No conclusion can be made about the performance of the geogrid reinforced base as the lane failed at the surface.

Are stone stabilized subbases a feasible alternative to the other limestone configurations relative to strength, performance, and cost?

The stone stabilized subbase performed as if it were a flexible pavement layer with an AASHTO layer coefficient of 0.10. This result must be regarded as tentative until further data is available from future trials. However, it implies that an adequate pavement could be constructed by substituting a 40 percent greater thickness of stone stabilized subbase for crushed limestone base. Note that an adequate thickness of the better quality crushed limestone base should be retained in any design using stone stabilized subbase to provide high strength support to the asphalt layers.

What are the relative strength and performance differences between pavements constructed on bases tested during this phase, as compared to the bases constructed during the other phases, when subjected to accelerated loading?

An answer to this question must await completion of tests on lanes 5 -10.

RECOMMENDATIONS

An investigation of the high dynamic impact of the ALF wheel meeting the pavement should be conducted with a view to possible future replacement of the current mechanical load control with a feed-back controlled hydraulic system.

A limited evaluation of the use of H-bar gages should be incorporated in the remaining Phase II tests, but in future test pavements less resource should be directed to strain measurement.

The potential for in pavement deflection measurement and for surface deflection measurement under full wheel load should be considered for future tests to supplement the strain measures.

Instrumentation for the measurement of moisture presence and pressure should be sought and incorporated in future tests.

After completion of loading of Phase II test lanes (5, 6, 7) and if there is a pause before starting testing of the second experiment, ALF should be repositioned on a new section of lane 3 and the test repeated. Any opportunity to repeat the loading of any lane should be pursued.

Data collection and processing procedures must take a higher priority to reduce, to the very minimum, gaps in the records.

Consideration should be given to providing subsoil drainage for the second experiment to reduce the influence of moisture fluctuation on the performance of the test lanes.

The Department should adopt a layer coefficient of 0.10 for stone stabilized soil base as an interim measure. Any pavement built using this material should be carefully monitored in comparison to a control section of full depth crushed stone base to further evaluate this coefficient.

The Department should adopt the equation

$$PSI = 5 - 0.0025 (ESAL = s \times 10^{-3})$$

for the prediction of performance of full-depth, crushed stone flexible pavements in PMS applications.

REFERENCES

1. Metcalf J.B. 1997 *The Application of Full Scale Accelerated Pavement Testing*, NCHRP Synthesis 235, Transportation Research Board, National Research Council, Washington, DC.
2. King, W., *Construction and Comparison of Louisiana Conventional and Alternative Base Courses under Accelerated Loading - Construction Report*, LTRC Report 93-1 ALF, Interim Draft, Louisiana Transportation Research Center, Baton Rouge, 1997.
3. Shahin M.Y., *Pavement Management for Airports, Roads and Parking Lots*, Chapman and Hall, New York, 1994.
4. SHRP, *Manual for FWD Testing in the Long-Term Pavement Performance Program*, SHRP Protocol P-661, Strategic Highway Research Program, National Research Council, Washington, D.C., 1993.
5. Scullion T. and C. Michalak, *MODULUS 4.0, Users Manual*, Report FHWA/TX-88/1123-4, Texas Transportation Institute, Texas A&M University, College Station, Texas, January 1991.
6. Roberts F.L. and J.B. Wedgeworth, *Analysis and Evaluation of Methods for Backcalculations of M_R values* - L.T.R.C. Report Nr. 263, Vol.1, LTRC, Baton Rouge, Louisiana, August 1992.
7. SHRP, *SHRP Layer Moduli Backcalculation Procedure*, SHRP Protocol P-655, Strategic Highway Research Program, National Research Council, Washington, D.C., 1993.
8. Ullitz P., *Pavement Analysis*, Elsevier, New York, 1987.
9. Jameson G.W., *Development of Procedures to Predict Structural Number and Subgrade Strength from Falling Weight Deflectometer Deflections*, November 1993.
10. A.A.S.H.T.O., *AASHTO Guide for Design Of Pavement Structures*, American Association of State Highway and Transportation Officials, Washington, D.C., Chapter II, 1993, page II-17--II-25.
11. Newcomb D.E., *Comparison of field and laboratory estimated resilient moduli of pavement materials*, Proceedings of the Association of Asphalt Paving Technologists, Vol.56, (1987), pp.91-110.
12. Lytton, Germann and Chou, *PASELS - Determination of Asphaltic Concrete Pavement Properties by Nondestructive Testing*, Appendix H, Texas Transportation Institute,

- College Station, Texas, February 1990.
13. Groendijk J., Vogelzang C. H. Miradi A., Molenaar A.A.A. and Dohmen L. J. M. , *Results of the LINTRACK Performance Tests on a Full-Depth Asphalt Pavement*, Transportation Research Board, 76 Annual Meeting, January 12-16, 1997, Washington, D.C.
 14. Rada G.R., Witczak M.W. and S.D.Rabinow, *Comparison of AASHTO Structural Evaluation Techniques Using Nondestructive Deflection Testing*, Transportation Research Record 1207, Transportation Research Board, Washington, D.C., 1988.
 15. Temple W.H. and R.W. Kinchen, *Asphaltic Concrete Overlays of Rigid and Flexible Pavements*, Final Report, La HPR Study No.69-3B, Louisiana Department of Transportation and Development, Baton Rouge, Louisiana, October 1980.
 16. Jameson G.W., Sharp G.B., Vertessy N.J., *A Full-Depth Asphalt Pavement Fatigue under Accelerated Loading* . 7th International Conference on Asphalt Pavements, 1994

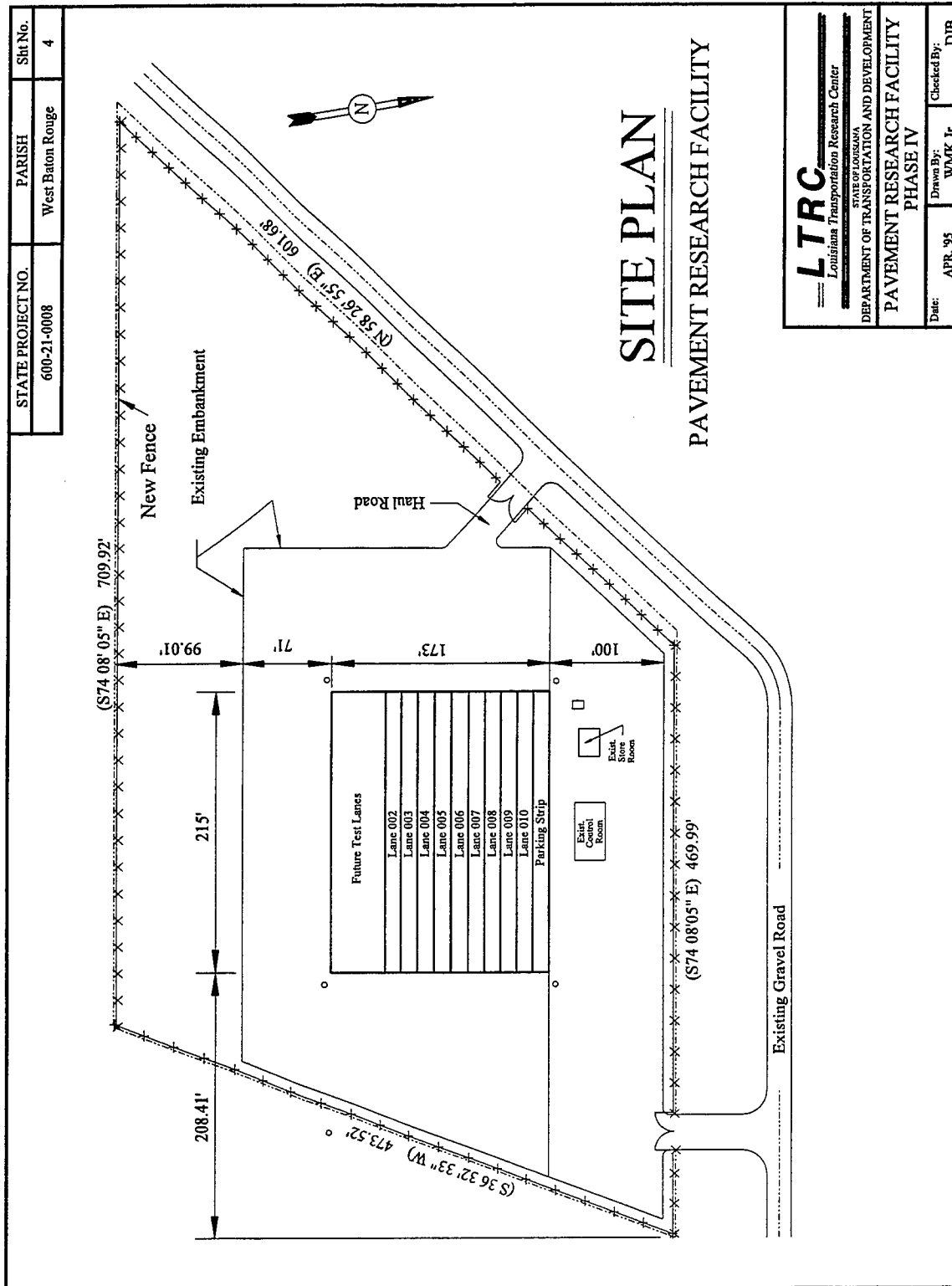


Figure 1
Plan of pavement research facility site

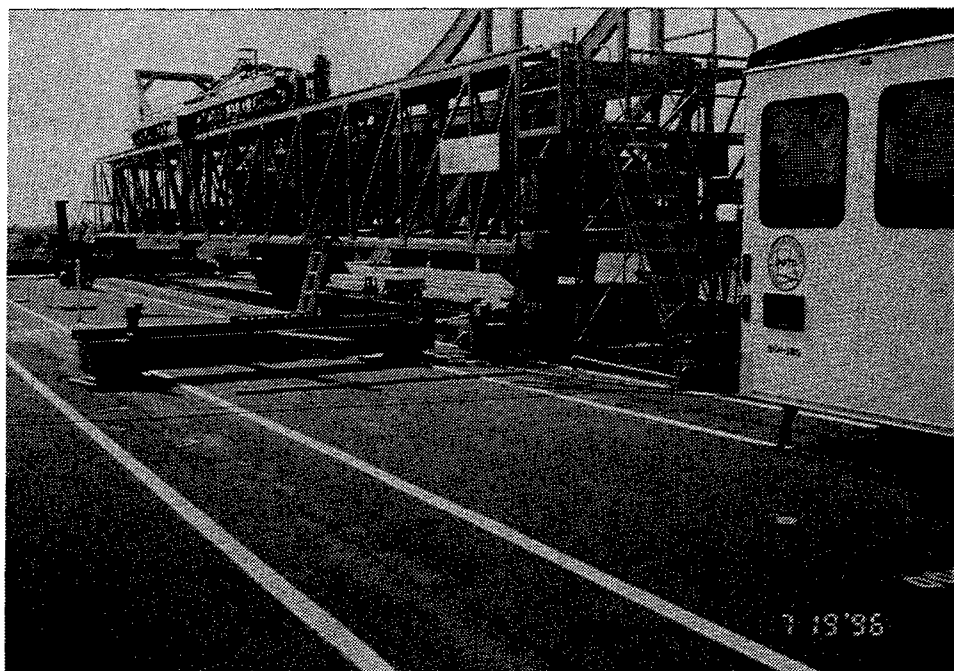


Figure 2
The Accelerated Loading Facility (ALF)

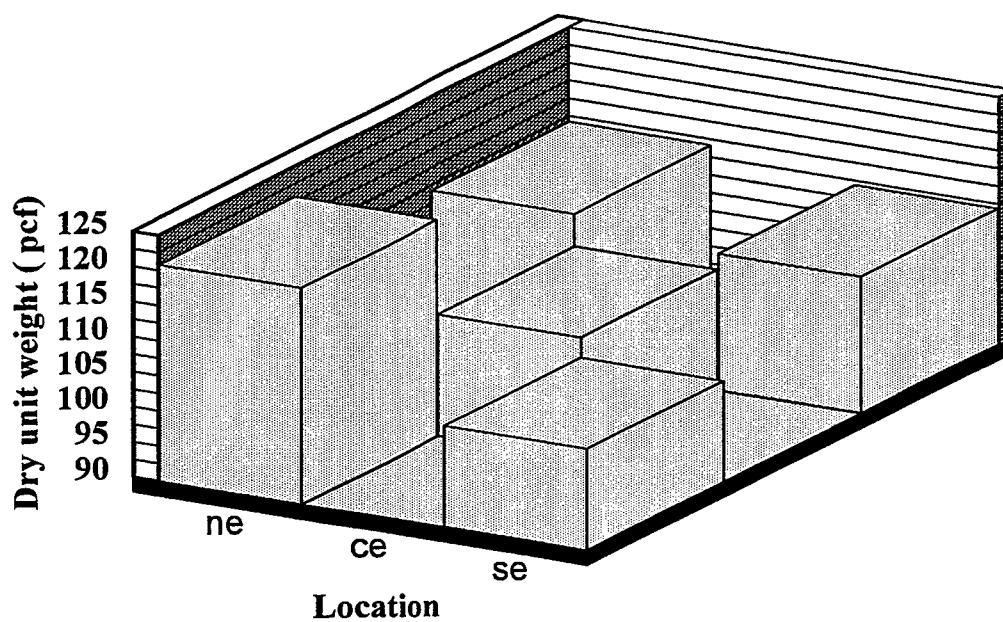


Figure 3
Embankment density contours

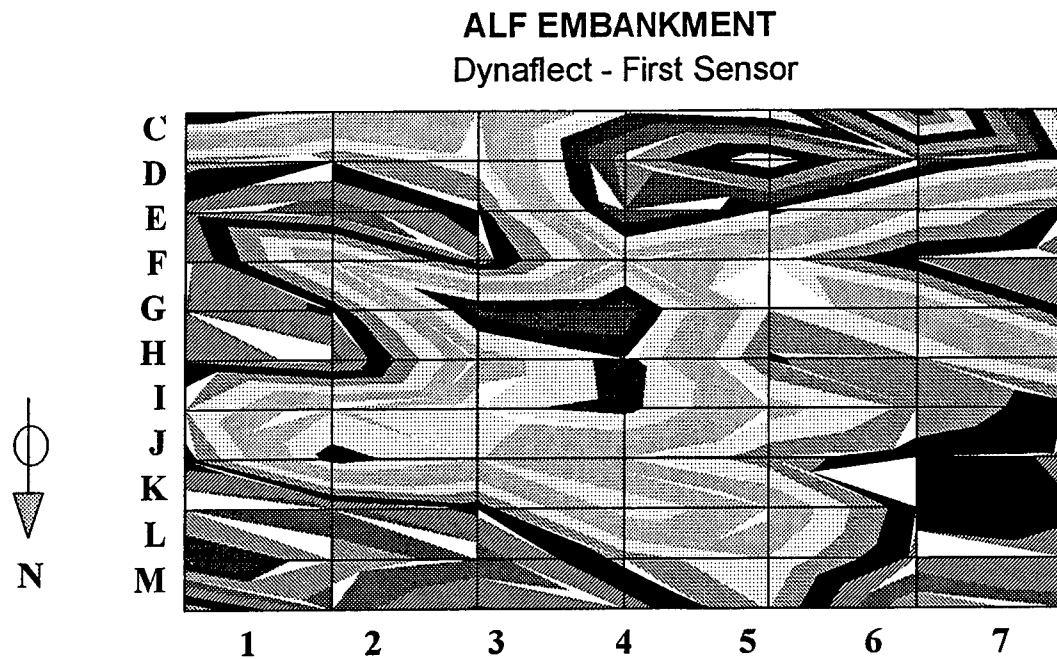


Figure 4
Embankment Dynalect deflection contours

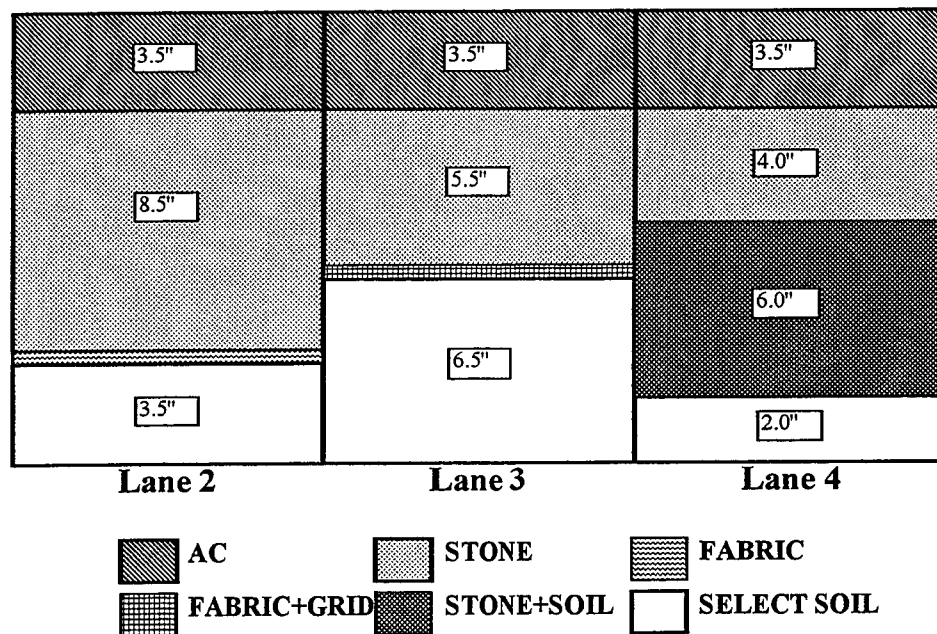


Figure 5
Pavement layer configuration -- Phase I

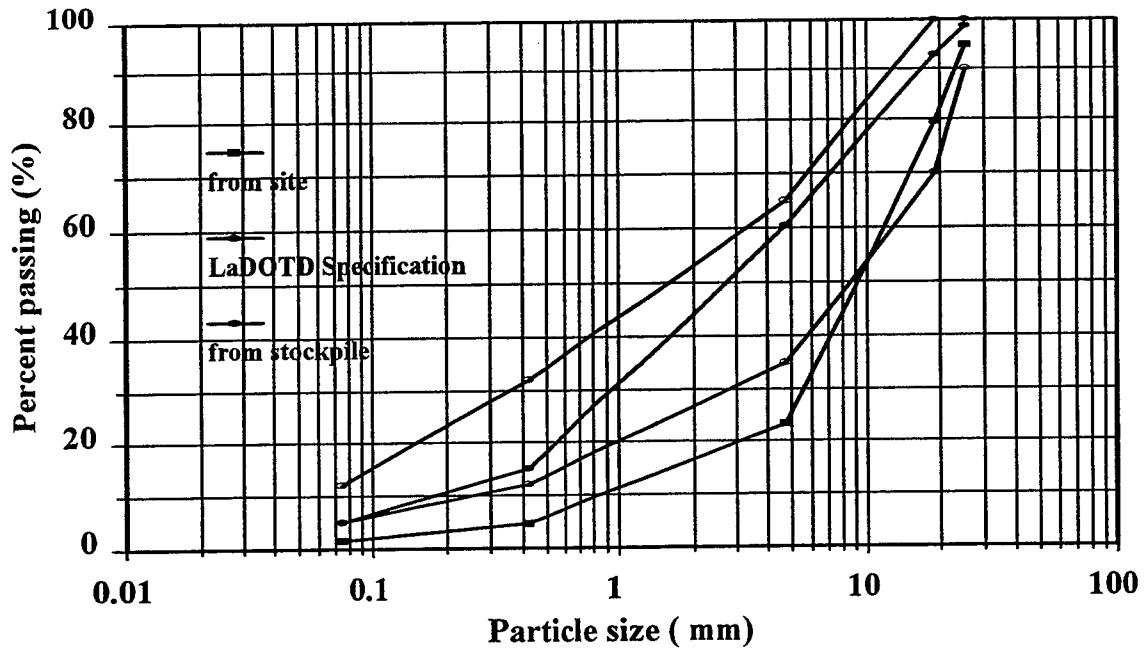


Figure 6
Base course gradation -- Phase I (as built)

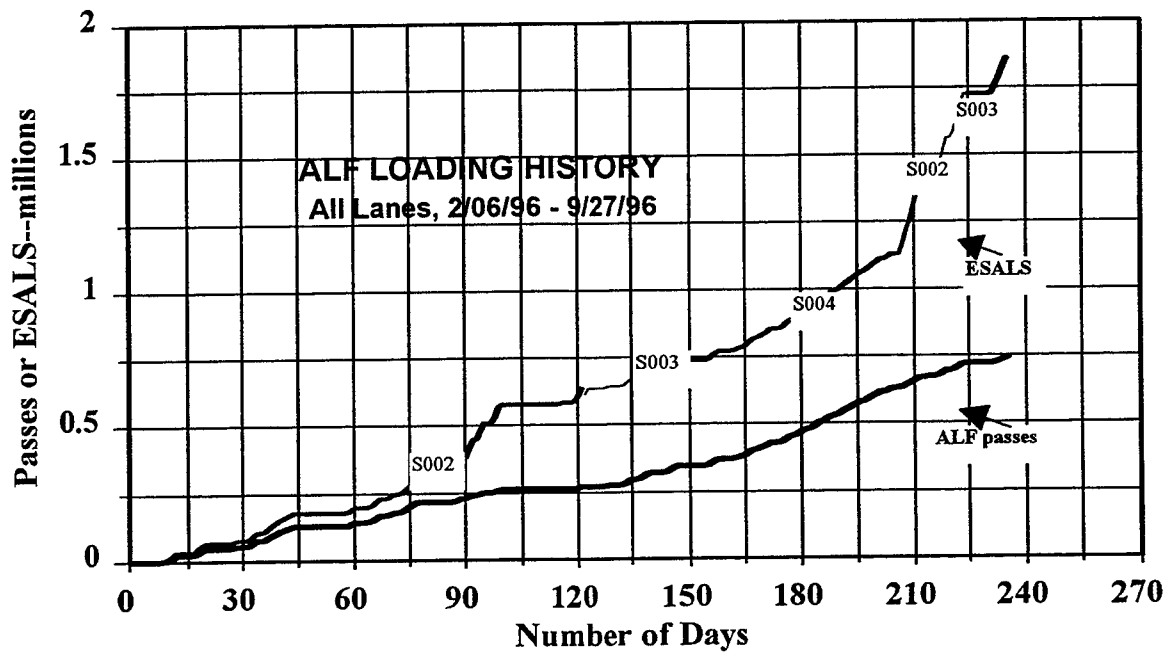


Figure 7
ALF loading history

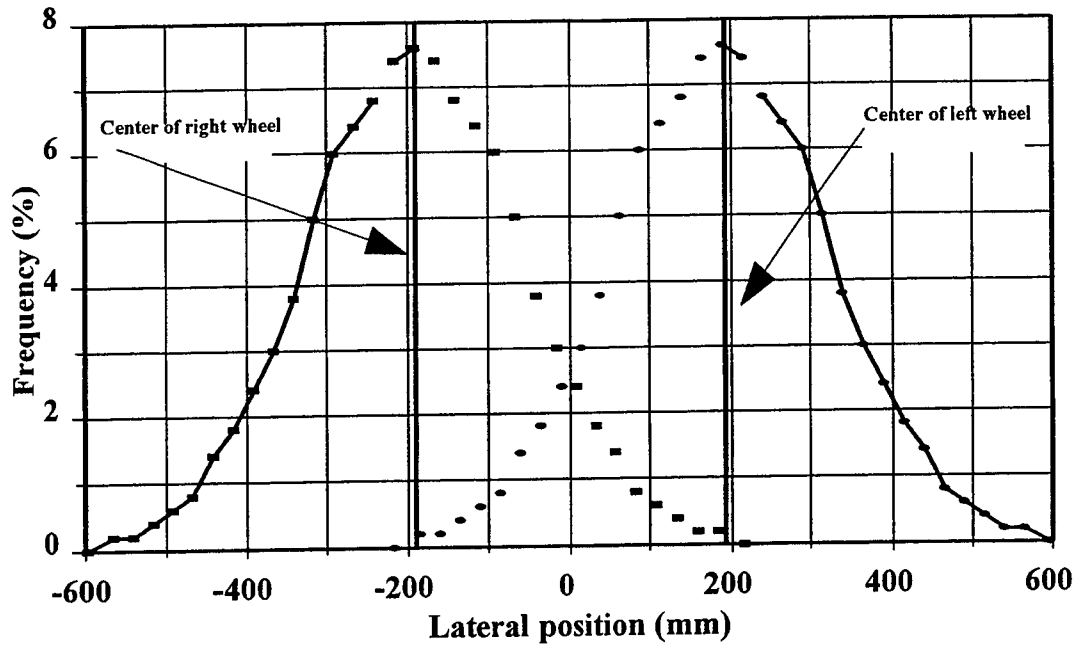


Figure 8
Transverse load distribution

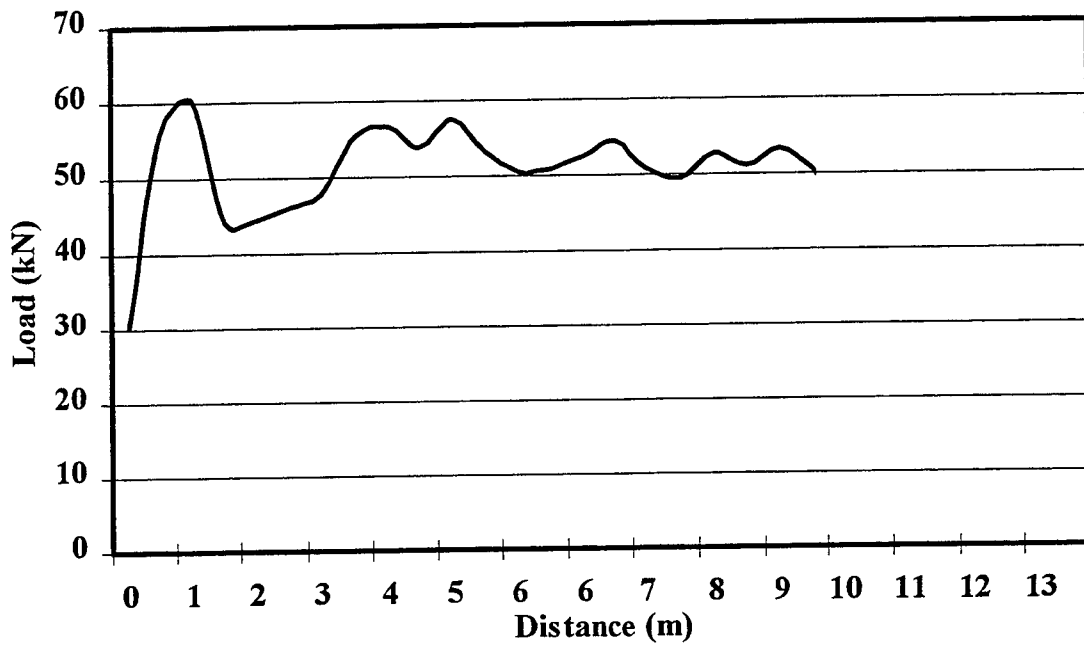


Figure 9
Longitudinal load distribution

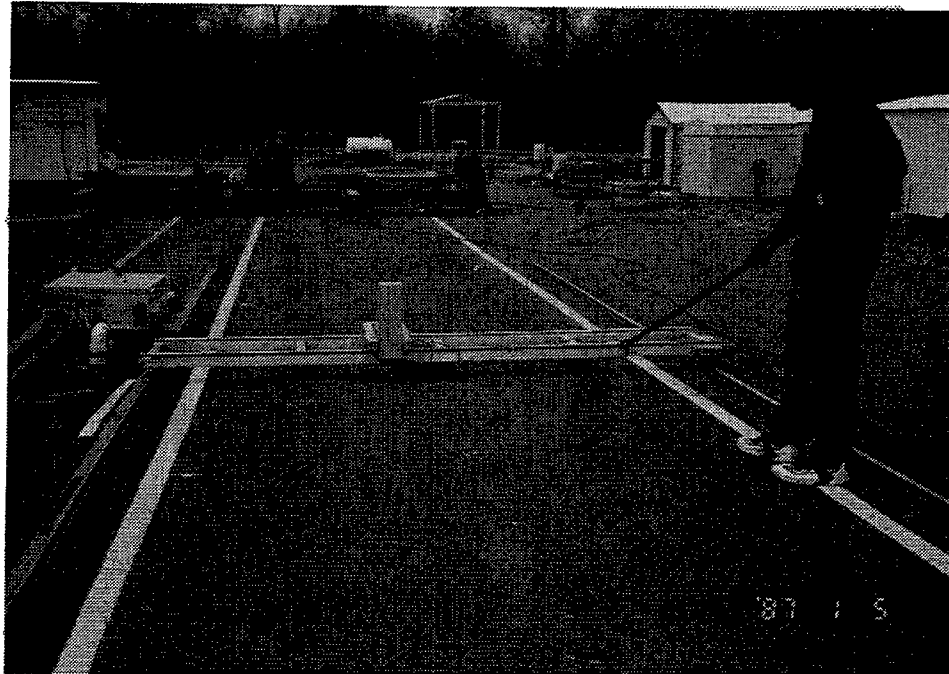


Figure 10
Pavement profile measurement

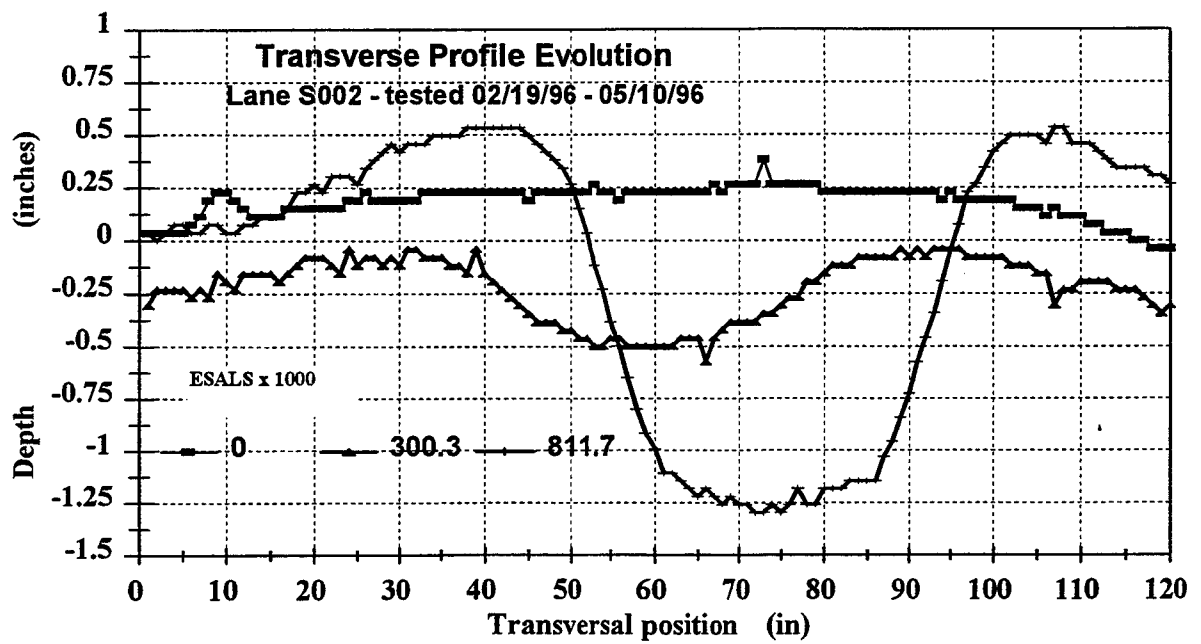


Figure 11
Typical transverse profiles

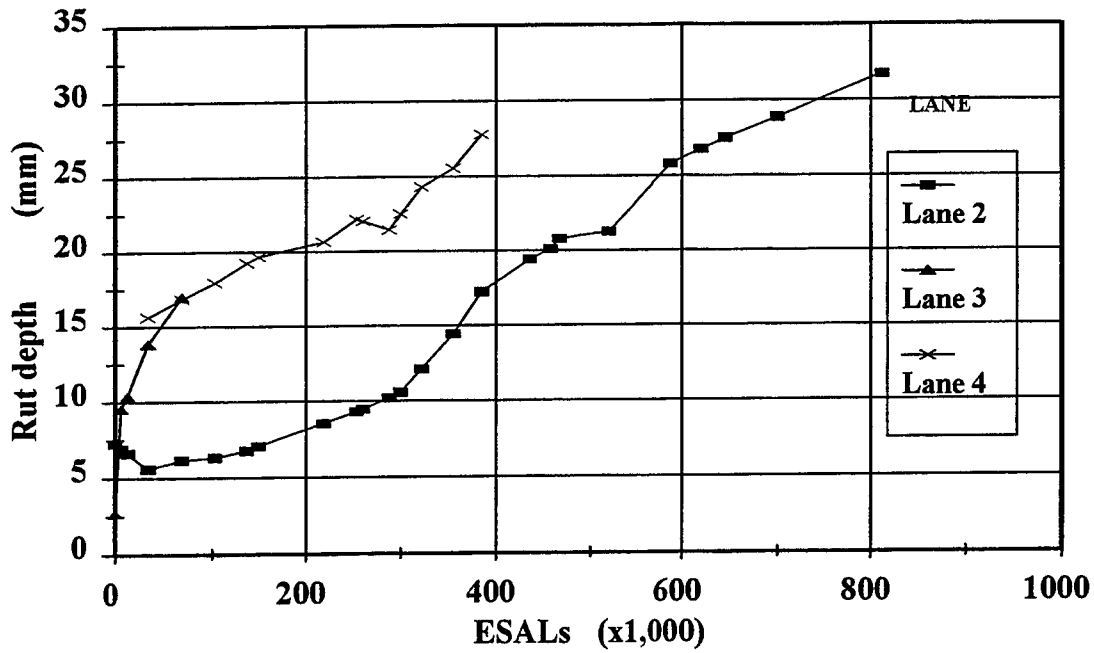


Figure 12
Development of rut depth

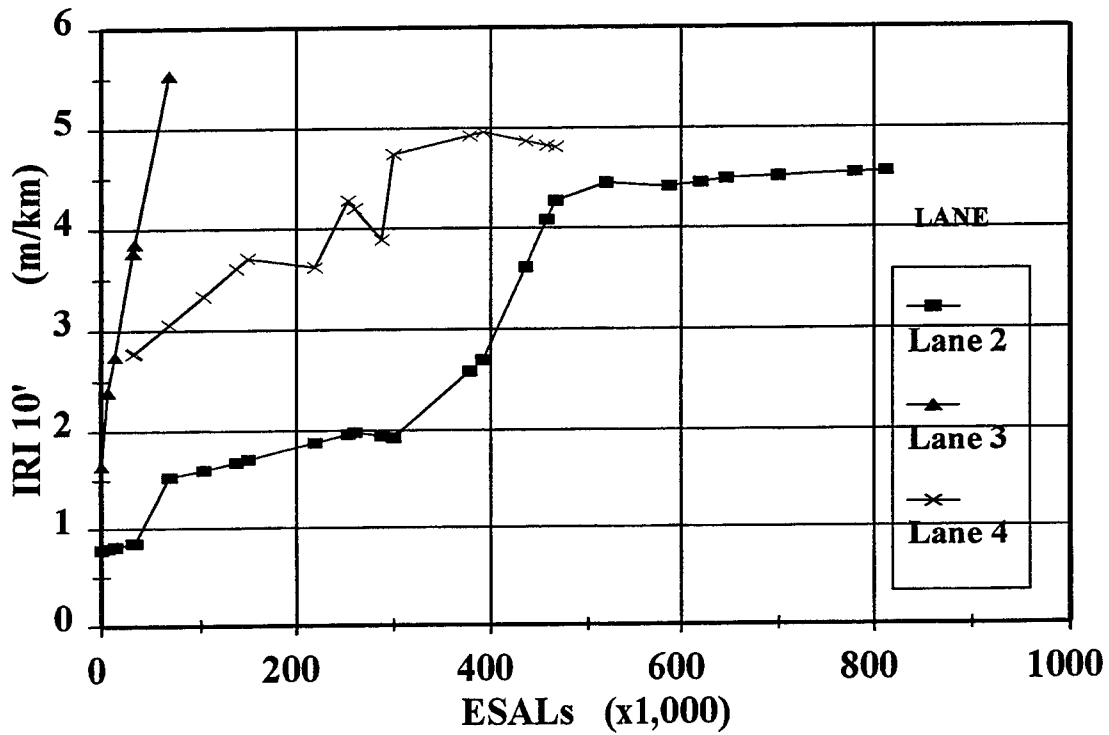


Figure 13
Development of roughness



Figure 14
Cracking measurement

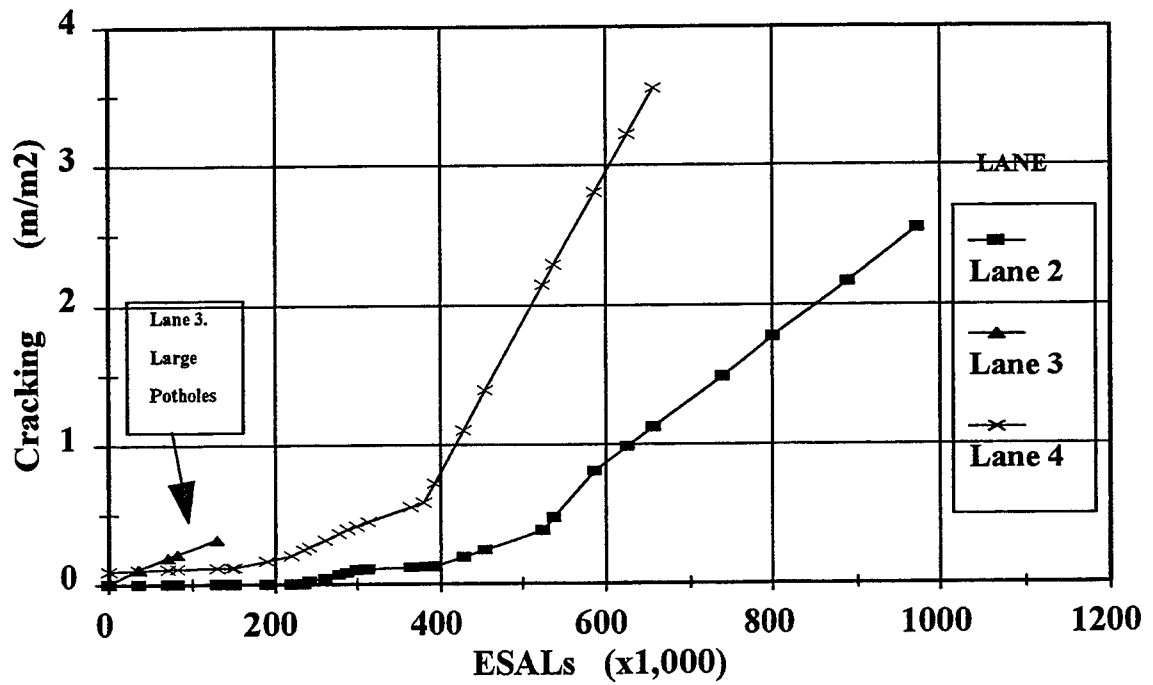


Figure 15
Crack development

Cracking Development to Failure

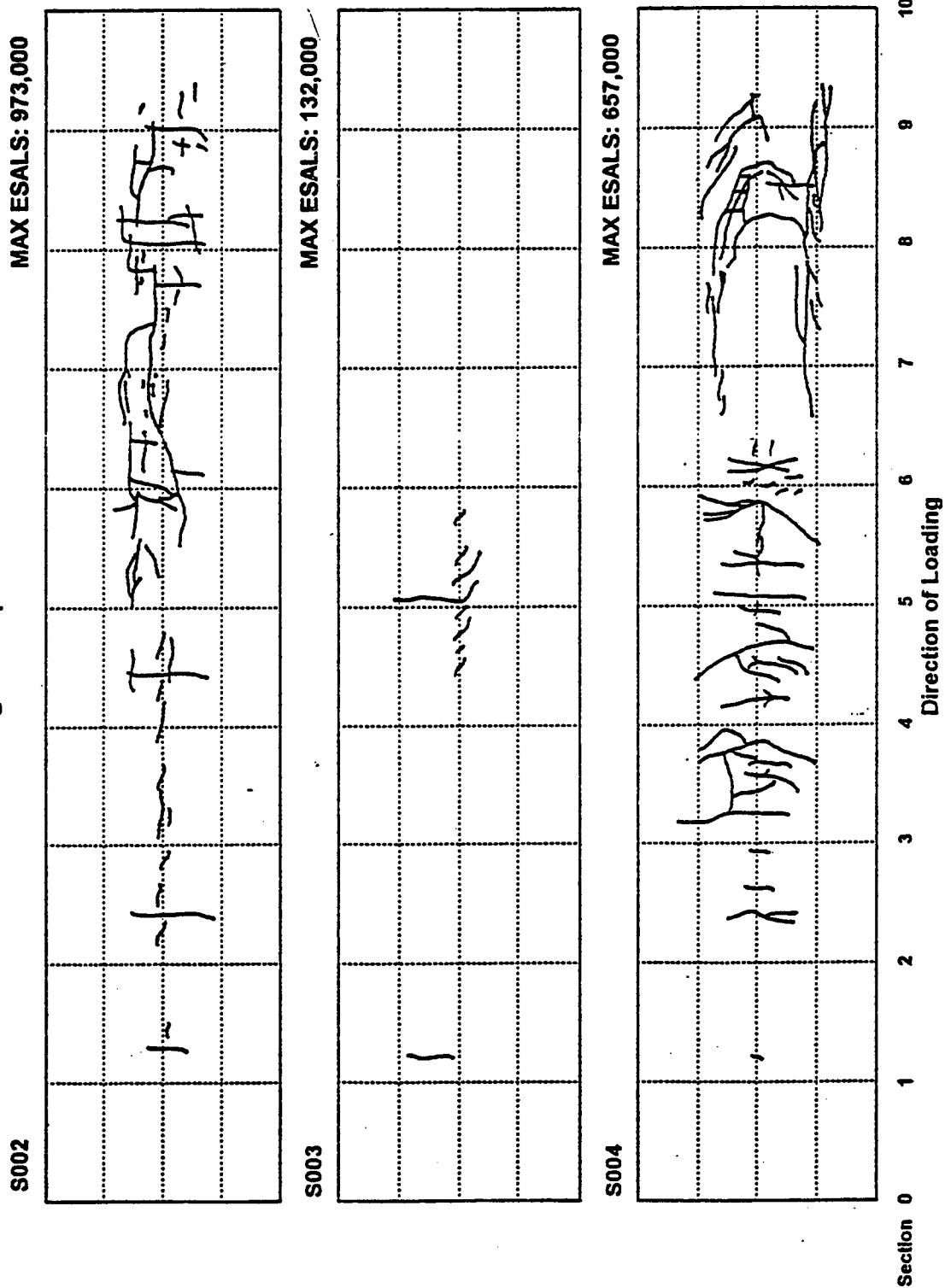


Figure 16
Crack patterns

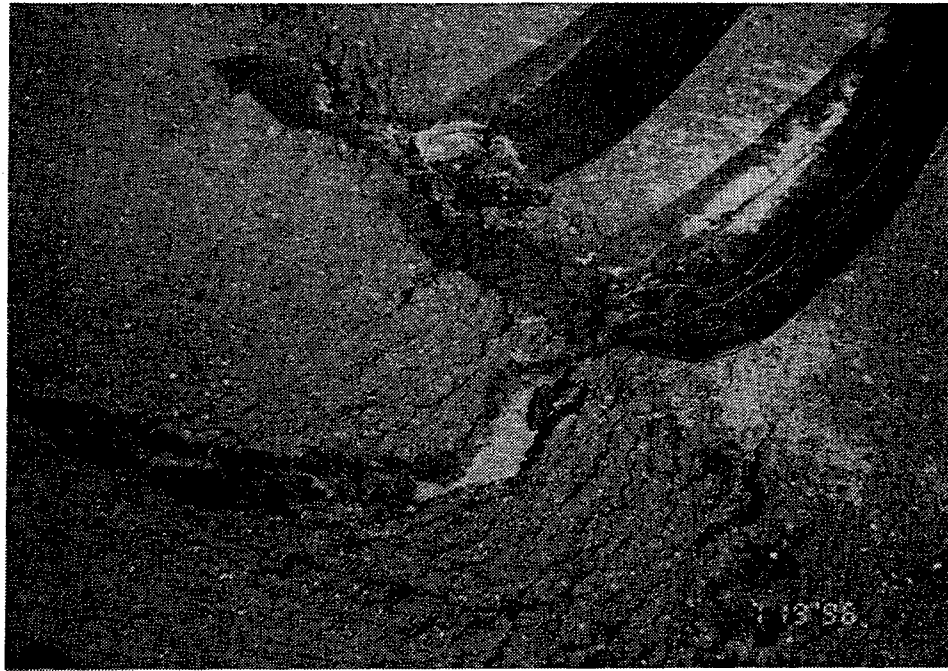


Figure 17
Pavement slippage failure - lane 3

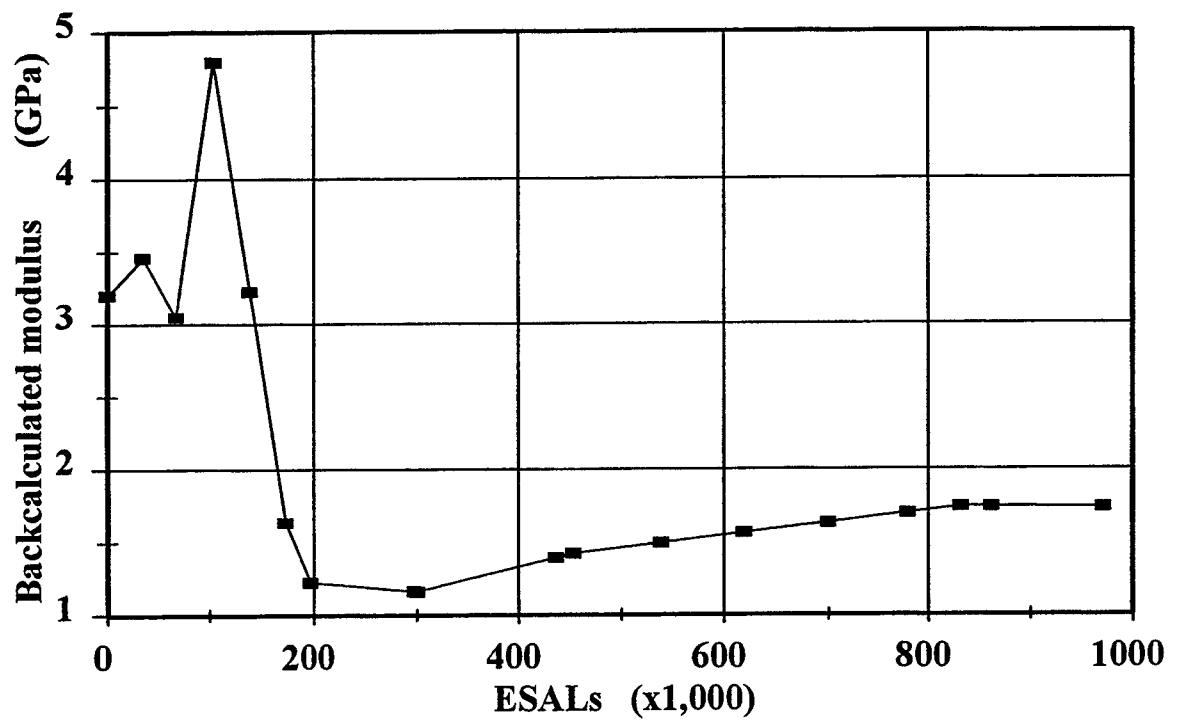


Figure 18
Average FWD back-calculated moduli - lane 2

ALF TEST BED PLAN VIEW (GAUGE INSTALLATION)

Figure 20

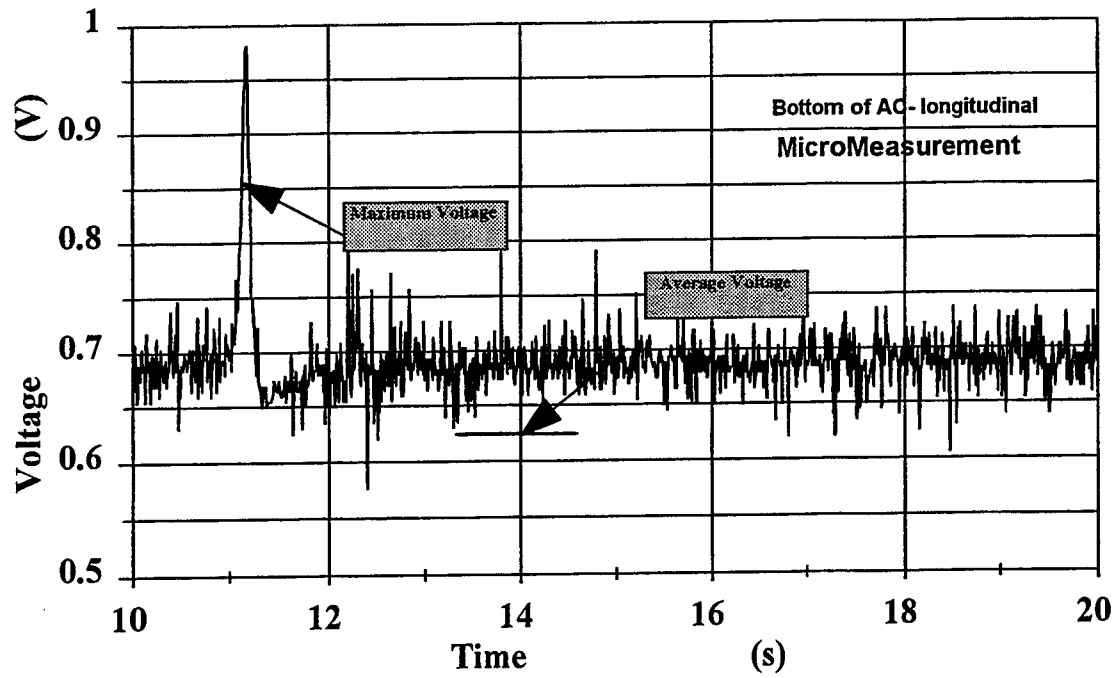


Figure 21
Typical strain signal trace

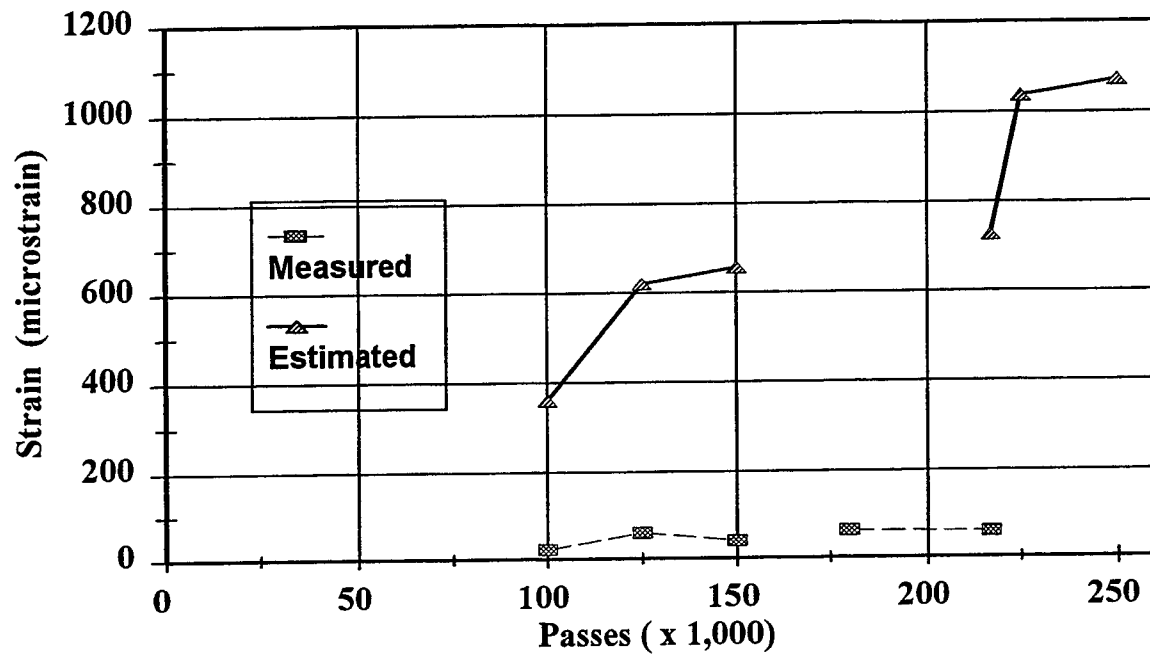


Figure 22
Discrepancy between estimated and measured strains

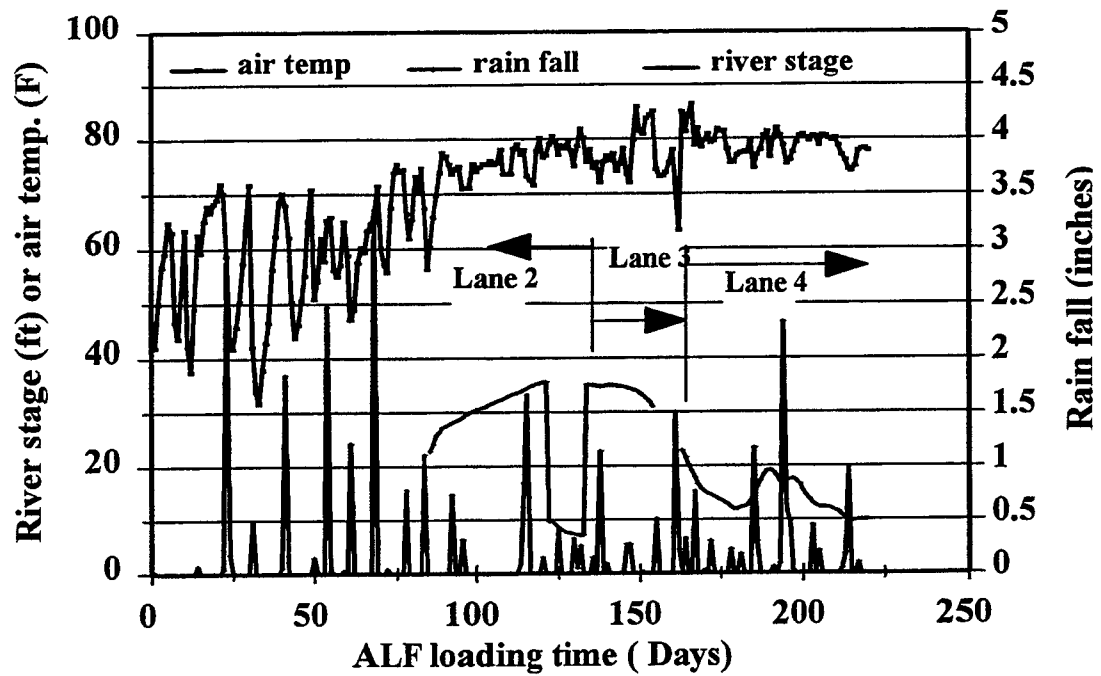


Figure 23
Daily temperature, rainfall, and Mississippi river stages

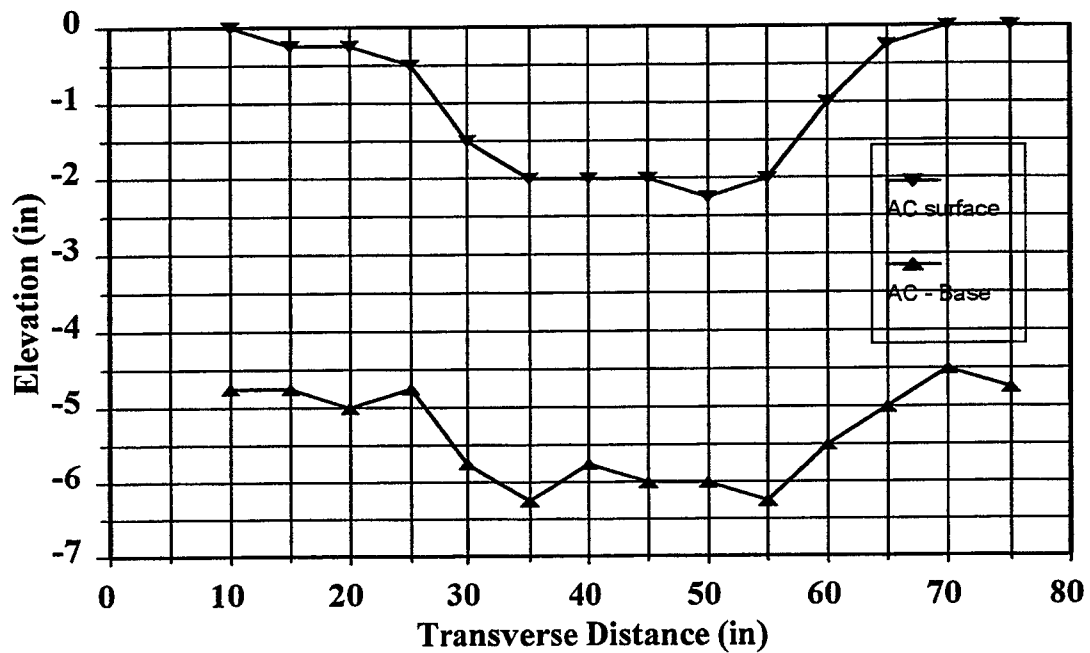


Figure 24
Post-mortem profile -- lane 2

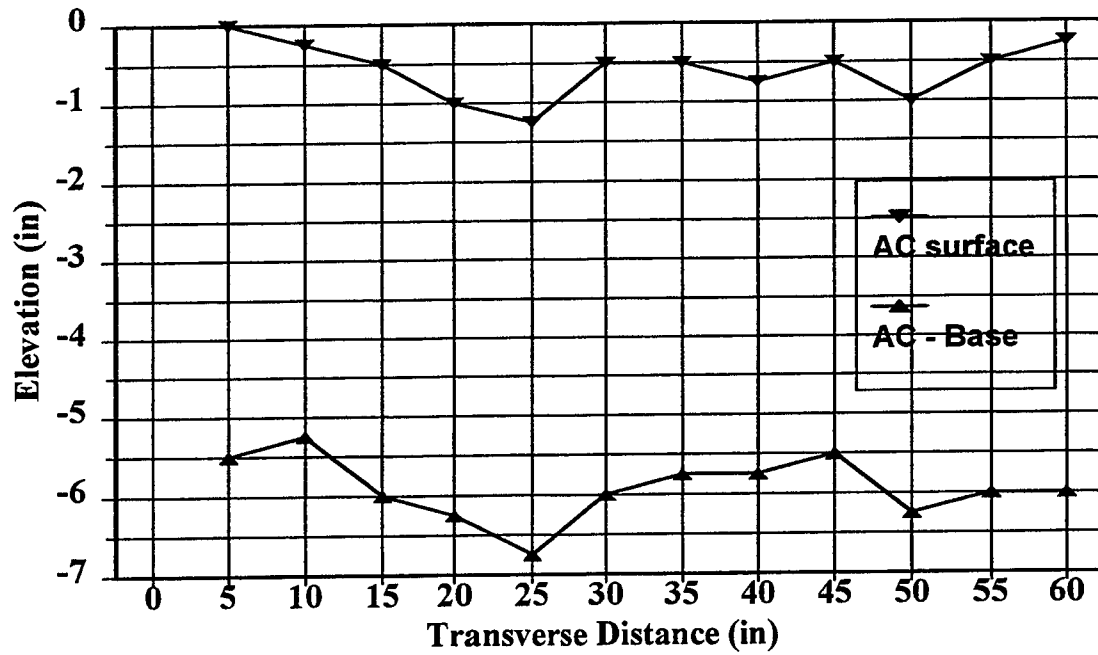


Figure 25
Post-mortem profile -- lane 3

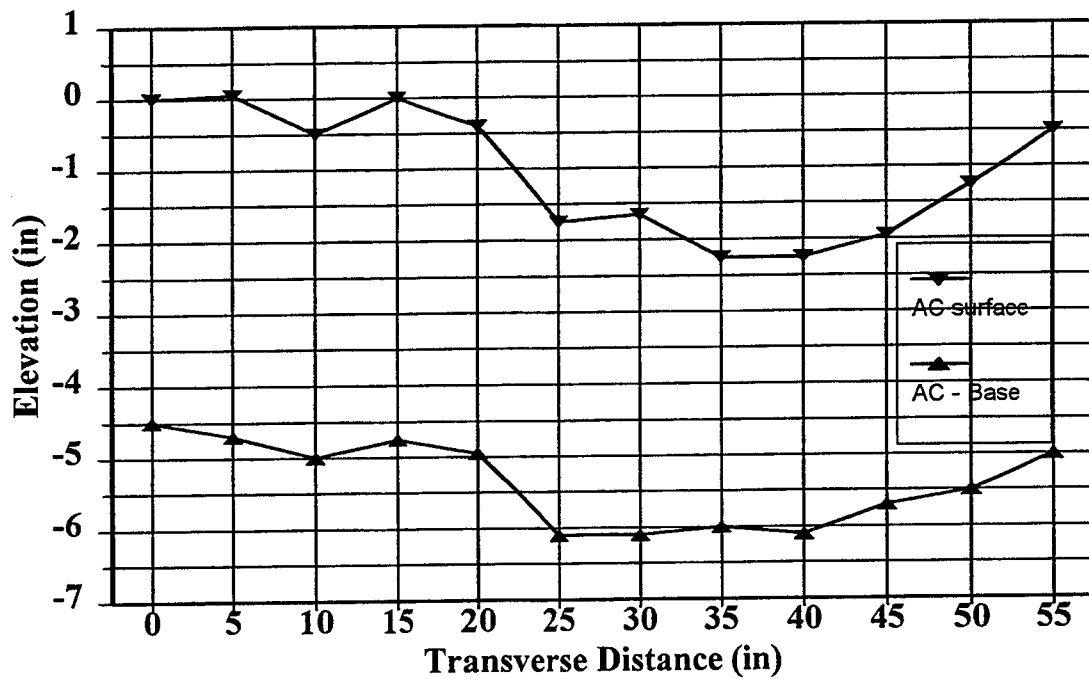


Figure 26
Post-mortem profile -- lane 4

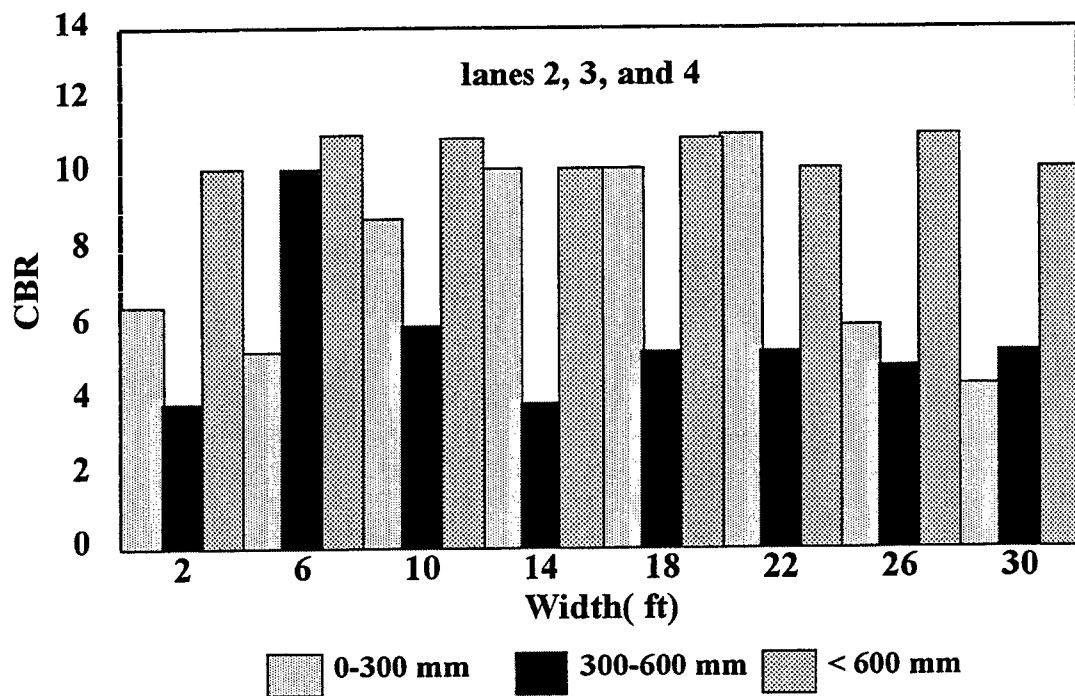


Figure 27
CBR below the subgrade surface (after post-mortem)

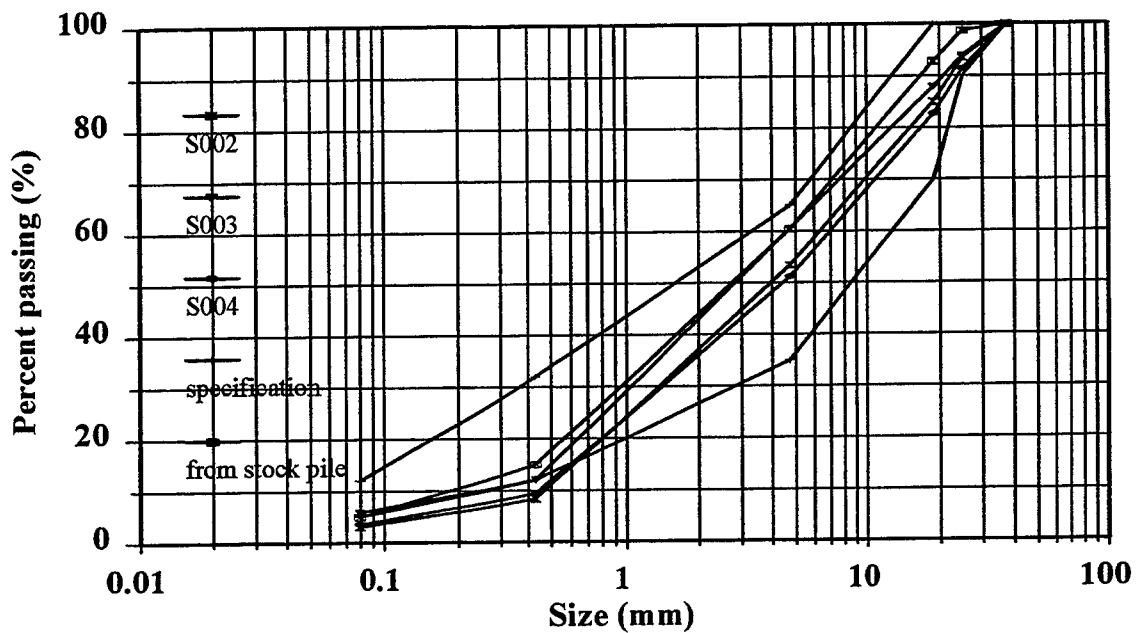


Figure 28
Gradation of crushed stone base layers after loading



Figure 29
Gages installed in lane 2 (after post mortem)

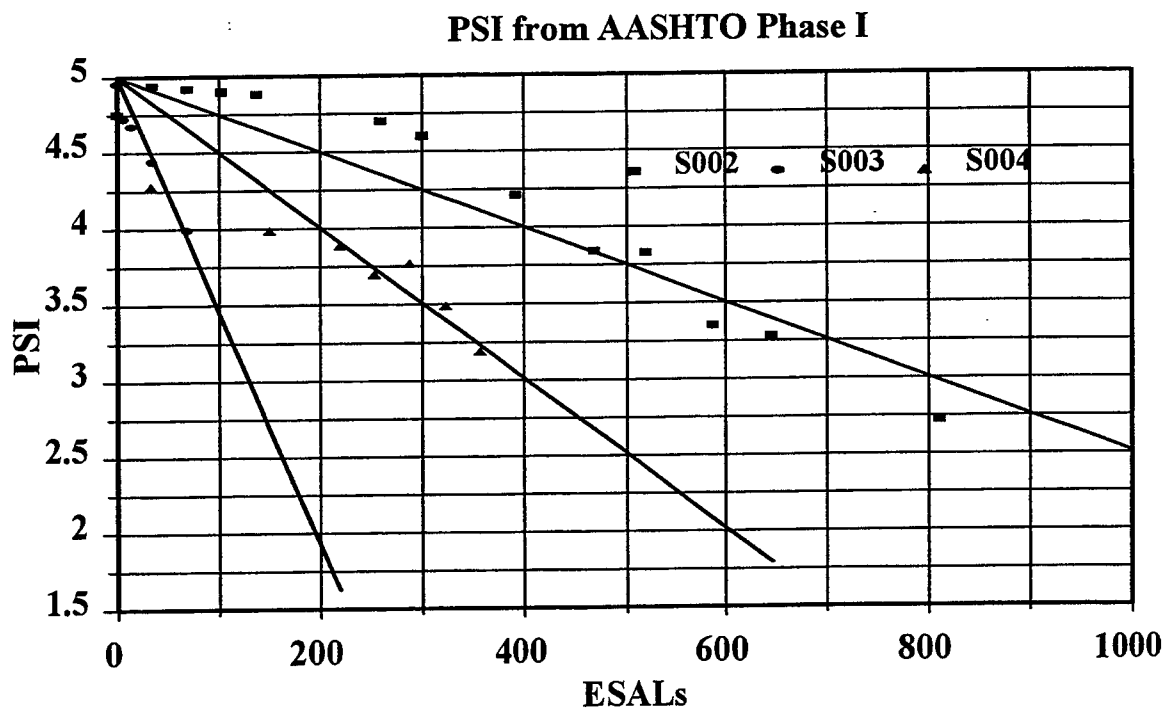


Figure 30
PSI and ESALs relationship for lane 2, 3, and 4

This public document is published at a total cost of \$1025.82. Two hundred copies of this public document were published in this first printing at a cost of \$665.82. The total cost of all printings of this document including reprints is \$1025.82. This document was published by Louisiana State University, Graphic Services, 3555 River Road, Baton Rouge, Louisiana 70802, to report and publish research findings of the Louisiana Transportation Research Center as required by R.S. 48:105. This material was printed in accordance with standards for printing by State Agencies established pursuant to R.S. 43:31. Printing of this material was purchased in accordance with the provisions of Title 43 of the Louisiana Revised Statutes.